Novel Retinoic Acid Metabolism Blocking Agents Endowed with Multiple Biological Activities Are Efficient Growth Inhibitors of Human Breast and Prostate Cancer Cells in Vitro and a Human Breast Tumor Xenograft in Nude Mice

Jyoti B. Patel,[†,‡] Carlic K. Huynh,[†,‡,§] Venkatesh D. Handratta,[†] Lalji K. Gediya,[†] Angela M. H. Brodie,[†] Olga G. Goloubeva,[∥] Omoshile O. Clement,[⊥] Ivo P. Nanne,[#] Dianne Robert Soprano,[▽] and Vincent C. O. Njar*[,†]

Department of Pharmacology and Experimental Therapeutics, University of Maryland School of Medicine, Baltimore, Maryland 21201-1559, Program in Toxicology, University of Maryland School of Medicine, 10 South Pine Street, MSTF 7-34F, Baltimore, Maryland 21201-1559, Biostatistics Division, University of Maryland Greenebaum Cancer Center, Baltimore, Maryland 21201-1559, Accelrys, 9685 Scranton Road, San Diego, California 92121, Department of Pharmaceutical Sciences, Temple University School of Pharmacy, 3307 North Broad Street, Philadelphia, Pennsylvania 19140, and Department of Biochemistry and Fels Institute of Cancer Research & Molecular Biology, Temple University School of Medicine, 3400 North Broad Street, Philadelphia, Pennsylvania 19140

Received July 23, 2004

Novel retinoic acid metabolism blocking agents (RAMBAs) have been synthesized and characterized. The synthetic features include introduction of nucleophilic ligands at C-4 of *all-trans*-retinoic acid (ATRA) and 13-*cis*-retinoic acid, and modification of terminal carboxylic acid group. Most of our compounds are powerful inhibitors of hamster liver microsomal ATRA metabolism enzyme(s). The most potent compound is methyl (2*E*,4*E*,6*E*,8*E*)-9-(3-imidazolyl-2,6,6-trimethylcyclohex-1-enyl)-3,7-dimethylnona-2,4,6,8-tetraenoate (**5**) with an IC_{50} value of 0.009 nM, which is 666,667 times more potent than the well-known RAMBA, liarozole (Liazal, IC_{50} = 6000 nM). Quite unexpectedly, there was essentially no difference between the enzyme inhibitory activities of the two enantiomers of compound **5**. In MCF-7 cell proliferation assays, the RAMBAs also enhance the ATRA-mediated antiproliferative activity in a concentration dependent manner. The novel atypical RAMBAs, in addition to being highly potent inhibitors of ATRA metabolism in microsomal preparations and in intact human cancer cells (MCF-7, T47D, and LNCaP), also exhibit multiple biological activities, including induction of apoptosis and differentiation, retinoic acid receptor binding, and potent antiproliferative activity on a number of human cancer cells. Following subcutaneous administration to mice bearing human breast MCF-7 tumor xenografts, **6** (VN/14-1, the free carboxylic acid of **5)** was well-tolerated and caused significant tumor growth supression (∼85.2% vs control, $p = 0.022$). Our RAMBAs represent novel anticancer agents with unique multiple mechanisms of action. The most potent compounds are strong candidates for development as therapeutic agents for the treatment of a variety of cancers.

Introduction

Retinoids, natural and synthetic analogues of *all-trans*-retinoic acid (ATRA) play key roles in many biological functions, including induction of cellular proliferation, differentiation, and apoptosis as well as developmental changes.[1] ATRA exerts its activity through binding with transcription-regulatory factors, known as the retinoic acid receptors (RAR), of which there are three subtypes, RARα, -β, and -γ. ATRA and several synthetic retinoids are currently used in cancer differentiation therapy, cancer chemoprevention, and treatment of dermatological diseases. One of the most impressive effects of ATRA is on acute promyelocytic leukemia (APL). Treatment of many APL patients with high doses of ATRA results in complete remission.[2,3] However, the clinical use of ATRA in the treatment of cancers is significantly hampered by the prompt emergence of resistance, which is believed to be caused at least in part by increased ATRA metabolism.[4−6]

One of the strategies for preventing in vivo catabolism of ATRA is to inhibit the P450 enzyme(s) responsible for this process. Inhibitors of ATRA metabolism (also referred to as retinoic acid metabolism blocking agents, RAMBAs) may prove useful for the chemoprevention and/or treatment of various kinds of cancer[5,6] and also for the treatment of dermatological diseases.[7,8] The major pathway of metabolic deactivation of ATRA starts with hydroxylation at C-4 to form 4-hydroxy-ATRA, which is oxidized into 4-oxo-ATRA, which is further transformed into more polar metabolites.[9] The first and rate-limiting step in the process is catalyzed by a cytochrome P450 dependent 4-hydroxylase enzyme. Although several human CYPs have been shown to be capable of converting ATRA to more polar metabolites,

* Corresponding author. Phone: (410) 706 5885. Fax: (410) 706 0032. E-mail: vnjar001@umaryland.edu.
† Department of Pharmacology and Experimental Therapeutics, University of Maryland School of Medicine.
‡ These authors contributed equally to this work.
§ Program in Toxicology, University of Maryland School of Medicine.
∥ University of Maryland Greenebaum Cancer Center.
⊥ Accelrys.
Temple University School of Pharmacy.
▽ Temple University School of Medicine.

10.1021/jm0401457 CCC: $27.50
Published on Web 11/26/2004

Chart 1. Structures of Two Potent ATRA 4-Hydroxylase Inhibitors: R116010, [*S*-(*R*,*R*)]-*N*-[4-[2-(Dimethylamino)-1-(1*H*-imidazol-1-yl)-propyl]phenyl]-2-benzothiazolamine, and Compound **50**, 2-{4-[2-(8-Cyclopropyl-4,4-dimethylspiro[chromane-2,1′-cyclopropane]-6-yl)ethynyl]-2-fluorophenyl}acetic Acid

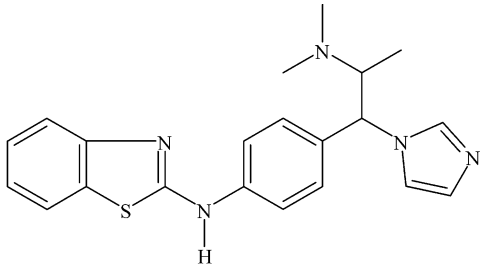

R116010

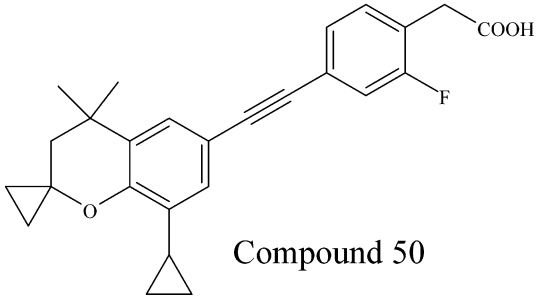

Compound 50

their specificity for ATRA is generally moderate. Recently, while CYP2C8 was reported to be a major contributor to ATRA 4-hydroxylation in the human liver,[10,11] Marill et al.[12] identified CYP3A7 as the most active enzyme responsible for ATRA metabolism. In addition, CYP26 has been identified as the most dedicated ATRA 4-hydroxylase.[13−17] CYP26 recognizes only ATRA as its substrate, and its expression and/or activity can be induced by ATRA both in vitro and in vivo. In adult humans, CYP26 is expressed in several tissues, mainly in liver, adrenals, heart, and hypophysis.[18] Perhaps of more significance to this work is the realization that a variety of human cancer cells and tumors have been shown to possess ATRA 4-hydroxylase activity.[19−26] *Irrespective of the CYP isozyme(s) involved*, increased metabolism of ATRA could generate a condition of retinoid (ATRA) deficiency, which is implicated in cancers and dermatological diseases. Agents that can prolong and intensify the action of endogenous ATRA by inhibiting ATRA metabolizing enzymes would have potential as clinical agents in the treatment of the aforementioned diseases.

Whereas several categories of nonretinoidal RAMBAs have been reported,[6,26−29] only a few retinoidal RAMBAs, developed by our group, are known.[6,30] Some RAMBAs reported by the Johnson & Johnson Pharmaceutical Research and Development group[7,26,27] (e.g. R116010, Chart 1) and those recently discovered by Allergan Sales Inc.[28] (e.g. compound **50**, a benzeneacetic acid derivative, Chart 1) are highly potent inhibitors, while those reported by the University of Cardiff group[29] are similar to ketoconazole (a weak inhibitor of ATRA-4-hydroxylase; cf. Table 1). As our approach to inhibition of ATRA metabolism enzyme(s), we have designed and synthesized substrate-like molecules with nucleophilic groups (e.g. azoles) at the 4-position of ATRA and of 13-*cis*-retinoic acid (13-CRA) (the major site of enzymatic hydroxylation). These substrate-like compounds not only are expected to interact with the ATRA-binding site of the enzyme, thus introducing high specificity, but also will provide a sixth ligand to the enzyme's heme iron, resulting in tight binding.[30] This paper describes the syntheses and in vitro and preliminary in vivo antitumor activity of novel azolyl retinoids. Several of these compounds, in addition to being potent RAMBAs, are endowed with potent antiproliferative, prodifferentiation, proapoptotic, and antitumor activities. A preliminary account of part of this work has already been published,[30] and two patents (US and World) are pending.

Table 1. In Vitro Inhibition of ATRA Metabolism in Hamster Liver and T47D Microsomes, and in Intact Breast Cancer Cells (MCF-7 and T47D)

	hamster liver microsomal assay		MCF-7 cells	T47D cells	
compd	IC_{50} (nM)[a]	K_i (nM)[b,c]	cellular assay: IC_{50} (nM)[a]	cellular assay: IC_{50} (nM)[a]	microsomal assay: IC_{50} (nM)[a]
5	0.009 ± 0.0007	4.60×10^{-5}	200.0 ± 2.50	215.0 ± 10.00	40.00 ± 3.00
(−)-**5**	−	−	−	6000.0 ± 32.00	680.00 ± 20.00
(+)-**5**	−	−	−	6000.0 ± 30.00	800.00 ± 25.00
6	2.33 ± 0.72	0.22	10.90 ± 0.52	6.3 ± 0.50	2.40 ± 0.12
7	2.00 ± 0.05	−	−	−	−
8	21.67 ± 0.30	−	−	−	−
9	5.84 ± 0.48	−	−	−	−
10	46.67 ± 3.30	−	−	−	−
11	0.050 ± 0.002	6.20×10^{-5}	24.70 ± 0.2	10.0 ± 0.60	5.20 ± 0.32
12	43.73 ± 4.70	0.35	56.00 ± 0.90	24.0 ± 0.2	−
13	61.25 ± 6.50	−	−	−	−
14	51.67 ± 4.40	−	−	−	−
15	23.00 ± 1.63	−	−	−	−
21	119.0 ± 20.2	4.12	−	−	−
22	57.50 ± 8.5	−	−	−	−
23	76.67 ± 13.36	0.78	−	−	−
for comparison:					
liarozole	6000.00 ± 30.00	−	ni	ni	−
ketoconazole	34000.00 ± 170	−	−	−	−
4-HPR	31850.00 ± 150	−	−	−	−

[a] Mean ± SDM of at least two experiments. [b] K_i values were determined as described in the Experimental Section. [c] K_m for substrate, ATRA = 160 nM; ni = no inhibition up to 10 μM; − = not determined.

Scheme 1. Synthesis of RAMBAs with ATRA Scaffold[a]

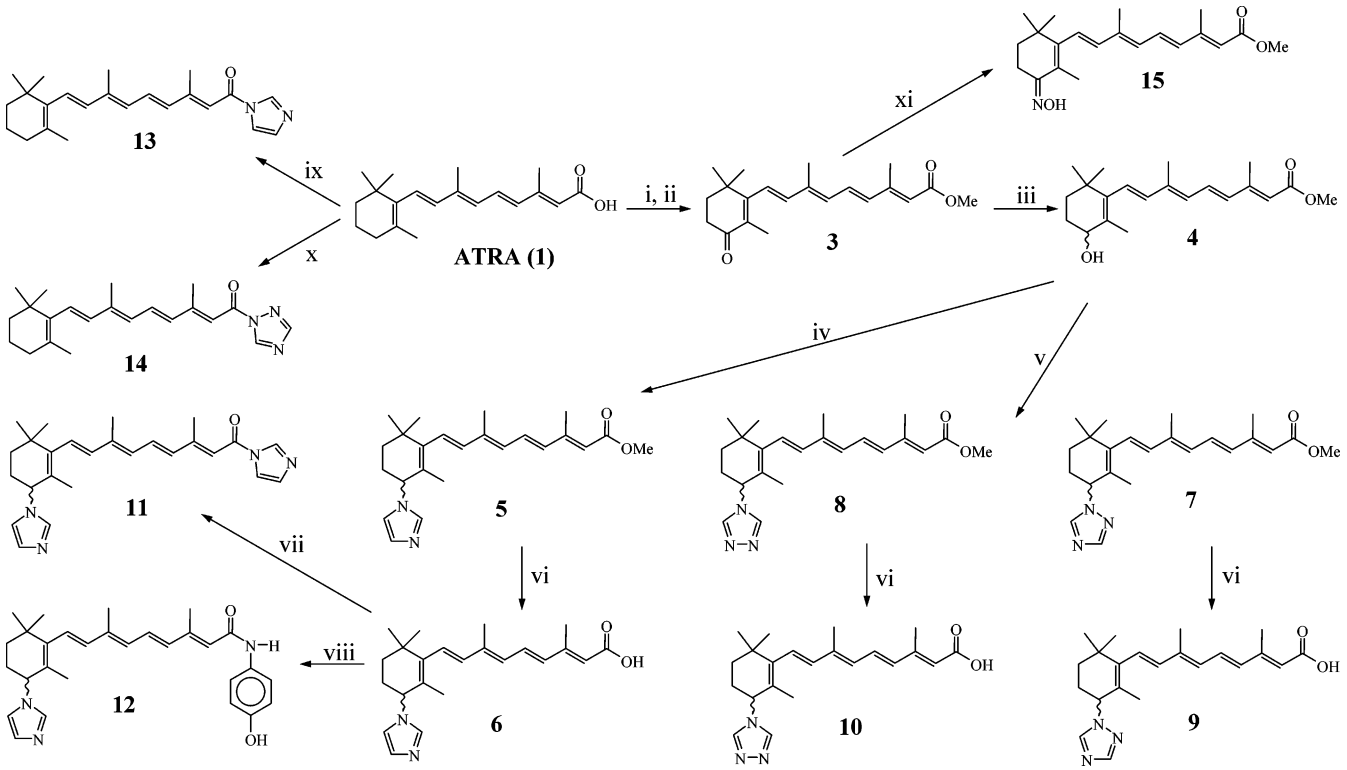

[a] Reagents and conditions: (i) $TMSCHN_2$/benzene, MeOH, Ar, rt; (ii) activated MnO_2/CH_2Cl_2, rt; (iii) $NaBH_4$/MeOH, rt; (iv) CDI/CH_3CN, rt; (v) CDT/CH_3CN, rt; (vi) 10% KOH/MeOH, Ar, reflux; (vii) CDI/CH_3CN, rt; (viii) DCC, HOBT, DMF, 4-APR; (ix) CDI/CH_3CN, reflux; (x) CDT/CH_3CN, reflux; (xi) $NH_2OH{\cdot}HCl$, NaOAc/EtOH, rt.

Chemistry

The azolyl compounds of this class of new RAMBAs were prepared in high yield in a four-step sequence (Scheme 1). Entry into the C-4 ATRA azoles started from ATRA (**1**) itself. Protection[31] of the carboxylic acid group as the methyl ester **2** followed by allylic oxidation[32] with MnO_2 provided the 4-oxo intermediate **3**, which was reduced with $NaBH_4$ to yield the key intermediate (±)-4-hydroxymethylretinoate (**4**). Treatment of **4** with carbonyldiimidazole (CDI) at room temperature gave the corresponding (±)-(1*H*-imidazol-1-yl)methylretinoate (**5**) in near quantitative yield. Alkaline hydrolysis of **5** resulted in (±)-(1*H*-imidazol-1-yl)retinoic acid (**6**) in 80% yield. The triazole derivatives, (±)-4-(1*H*-1,2,4-triazol-1-yl)methylretinoate (**7**) and (±)-4-(4*H*-1,2,4-triazol-4-yl)methylretinoate (**8**) were obtained as previously described by treatment of **4** with carbonylditriazole (CDT). Hydrolysis of **7** and **8** gave their corresponding free acids, (±)-4-(1*H*-1,2,4-triazol-1-yl)retinoic acid (**9**) and (±)-4-(4*H*-1,2,4-triazol-4-yl)-retinoic acid (**10**), respectively. The ease of transfer of imidazole and triazole from CDI and CDT, respectively, in excellent yields to the carbinol carbon of **4** are attributable to the activated nature of the allylic OH. It should be stated that transfer of imidazole from CDI to benzylic, vinylogous, and benhydryl carbinol carbons in modest to excellent yield has been previously reported.[33] Treatment of compound **6** with CDI at room temperature gave the 4-azolyl retinamide **11** in near quantitative yield, while the arylretinamide **12** was synthesized by coupling **6** with *p*-aminophenol (*p*-AP) by the active ester method using dicyclohexylcarbodiimide (DCC) and 1-hydroxybenzotriazole (HOBT). Retinamides **13** and **14** were also prepared by treatment of ATRA (**1**) with CDI or CDT, respectively. The 4-keto oxime (**15**) was synthesized in near quantitative yield by treatment of ketone **3** with hydroxylamine hydrochloride. The stereochemistry of the oxime **15** about the C=N bond was assigned the *E* geometry because the signal of the two C-3 hydrogens in the ^1H NMR spectrum shifted downfield to δ 2.74. This demonstrates that the oxime possesses the geometry in which the C-3 hydrogens are proximate to the oxime OH. That the downfield shifts of these two hydrogens are not simply attributable to the anisotropy of the exocyclic π system at C-4 is apparent from analysis of the ^1H NMR spectrum of the 4-oxo derivative **3**, in which the C-3 hydrogens appear relatively upfield at δ 2.52. RAMBAs with the 13-CRA scaffolds, compounds **21**, **22**, and **23** (Scheme 2), were also synthesized using reactions described above for the synthesis of corresponding RAMBAs with ATRA scaffolds, but starting from 13-CRA (**16**). Hitherto unreported ^{13}C NMR data for all compounds are presented in the Experimental Section. The ^{13}C NMR chemical shifts were assigned by comparison with reported values for closely related retinoids.[34, 35]

The 4-azole derivatives described in this paper are racemates. Because their enantiomers may show differences in enzyme inhibitory potencies, it was of interest to separate the enantiomers of our most potent inhibitor (racemate **5**, vide infra) for testing. Compound **5** enantiomers, (4*R*)-(−)- and (4*S*)-(+)-**5** (Figure 1), were readily separated by HPLC on a chiral column Chiralpak AD using UV detection. The chromatograms for racemate **5** and (4*R*)-(−)- and (4*S*)-(+)-**5** are presented

Scheme 2. Synthesis of RAMBAs with 13-CRA Scaffold[a]

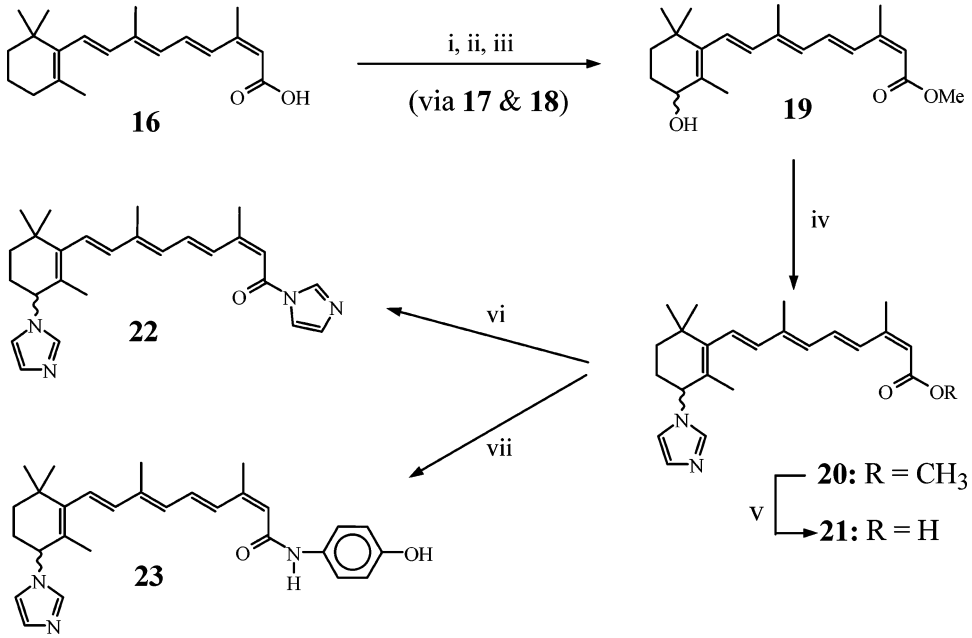

[a] Reagents and conditions: (i) $TMSCHN_2$/benzene, MeOH, Ar, rt; (ii) activated MnO_2/CH_2Cl_2, rt; (iii) $NaBH_4$/MeOH, rt; (iv) CDI/CH_3CN, rt; (v) 10% KOH/MeOH, Ar, reflux; (vi) CDI/CH_3CN, reflux; (vii) *p*-AP, HOBT, DMF, DCC.

in Figure 1. Tentative assignment of the chirality (absolute configuration) at C-4 of the two enantiomers was achieved on the basis of their optical rotations in comparison with the knowledge of the absolute configurations of related (4*S*)-(+)-4-hydroxyretinal and (4*R*)-(−)-4-hydroxyretinal.[36]

Biological Results and Discussion

Enzyme Inhibition Studies. A potent inhibitor of ATRA hydroxylases, the enzyme complex responsible for ATRA metabolism would be expected to increase the levels of endogenous ATRA, enhancing the "ATRA-mimetic" effects without the need for ATRA administration. In humans, the target enzymes involved in ATRA metabolism are the nonspecific liver CYPs, among which CYP2C8 and 3A7[10−12] are the major contributors, and the ATRA-inducible CYP26.[13−17] Although some investigators[7,26−28] have targeted inhibition of CYP26, it seems more realistic that both the nonspecific CYPs and specific CYP26 would need to be targeted since without initial ATRA accumulation due to nonspecific CYP action, ATRA levels would be insufficient to induce CYP26. Smith and co-workers[29] have also recently articulated this alternative strategy. With these considerations, we have tested our compounds against the more readily available hamster liver microsome and ATRA-induced CYP26 in MCF-7 and T47D breast cancer cells. It should be emphasized that several groups[22,24−26] have clearly demonstrated that CYP26 is the major ATRA-hydroxylating enzyme in both MCF-7 and T47D cells.

RAMBAs in Hamster Liver Microsomal Assays. The prospective inhibitors were evaluated using microsomal preparations of male hamster liver fortified with NADPH, using [11,12-^{3}H]-ATRA as substrate as we have previously described.[30a] The results are given as IC_{50} values (determined from dose response curves) and are presented in Table 1. All of our compounds exhibited potent inhibitory activity at nanomolar concentration with IC_{50} values of 0.009−119.00 nM. Our best compound **5** showed a 666,667-fold stronger inhibitory activity (IC_{50} = 0.009 nM) than liarozole (IC_{50} = 6000 nM), the only RAMBA to undergo phase III clinical studies in prostate cancer and in psoriasis. After careful evaluation in repeated assays, some of our compounds (i.e., **6**, **9**, and **10**) were found to be more potent inhibitors of hamster liver microsomes than our earlier tests indicated.[30a] As expected, compounds with the ATRA scaffold (**5**−**15**) were more potent than those with the 13-CRA scaffold (**21**−**23**). Furthermore, the results suggest that the nature of the C-4 substituent is important in determining affinity for the enzyme (compare IC_{50} values of **6**, **7**, **8** versus **13** and **14**; see Table 1) and also reveal that the corresponding methyl esters (**5**, **7**, and **8**) and imidazole amide (**11**) are significantly (24- to 48-fold) more potent than the corresponding free acids (**6**, **9**, and **10**). Compounds with 4-imidazole substitutions (**5**, **6**, and **11**) are the most potent three inhibitors. Thus, it would appear that the imidazolyl nitrogen lone pair makes the strongest coordination to the iron atom of the heme in the active site of the enzyme. Compound **12** (IC_{50} = 43.7 nM) was synthesized to determine the effect of increasing the size of the terminal amide group. The modification resulted in a considerable 875-fold decreased potency compared to **11** (IC_{50} = 0.05 nM), suggesting limited bulk tolerance at the active site of the enzyme. Because ketoconazole is used as a standard inhibitor of ATRA metabolism[10−12,26−29] and 4-HPR has recently been suggested as an inhibitor of ATRA metabolism,[37] we also tested these two compounds for comparison. As shown in Table 1, ketoconazole and 4-HPR are very weak inhibitors of this enzyme complex.

Following the determination of IC_{50} values, some seven representative inhibitors (**5**, **6**, **11**−**13**, **15**, and **21**) were evaluated further to determine their apparent

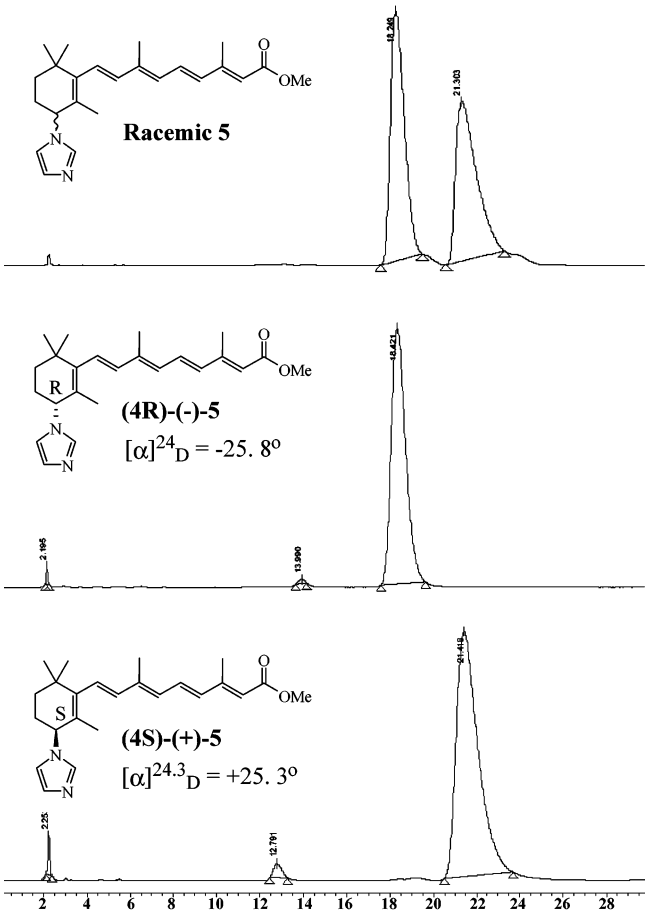

Figure 1. HPLC resolution of the enantiomers of (±)-**5** at 25 °C and structures of racemate **5** and its enatiomers. Conditions: column, Chiralpak AD (4.6 × 250 mm); eluent, hexane/isopropyl alcohol (95:5, v/v); flow rate, 1.5 mL/min. Chromatograms: top to bottom, UV detection, of racemic **5**, (−)-**5** (t_R = 18.42 min), and (+)-**5** (t_R = 21.42 min), respectively. Optical purity was determined by chiral HPLC (see above) and found to be >99.9% ee for both enantiomers.

K_i values (from Lineweaver−Burk plots, e.g. Figure A, Supporting Information) and also the type of enzyme inhibition kinetics. The apparent K_i values are presented in Table 1. Except for **12**, which exhibited uncompetitive-type inhibition (caused decrease in both V_{max} and K_m to the same extent), all other compounds were excellent noncompetitive-type inhibitors of the enzyme complex as shown in Figure A. The nature of inhibition kinetics exhibited by a majority of the compounds was that in which the V_{max} decreased but the apparent K_m was unchanged. This is one of the two characteristics of a noncompetitive enzyme inhibitor and indicates destruction of the catalytic activity of the enzyme.

Enzyme kinetic studies of ATRA metabolism revealed a K_m value of 160 nM, which is lower than the K_m values of 1.1 and 12.5 μM determined by Roberts et al.[38] and Van Wauwe et al.,[39] respectively. Nadin and Murray[10] and McSorley and Daly[12] reported K_m values of 9.0 and 0.9 μM, respectively, for human liver microsomes. It is not clear whether these different K_m values reflect real differences in affinity for ATRA between human and rodent ATRA hydroxylase. The conversion of ATRA to polar metabolites in hepatic microsomal preparations is catalyzed by more than one CYP, but with major contributions from CYPs 2C8, 2C9, 3A4, and 26. Therefore, the kinetic parameters reported in this manuscript do not represent the kinetics of a single enzyme. Our novel compounds are also expected to be potent inhibitors of human liver enzymes because the same CYP isoforms have also been identified as the major contributors in ATRA metabolism.

To the best of our knowledge, the most inhibitory compounds in the present study are far more potent than any inhibitor of ATRA metabolism for which comparable data have been previously described. The IC_{50} value for **5** was 0.009 nM, whereas the most potent inhibitor of yeast microsomes expressing CYP26 reported to date is R115866, with an IC_{50} value of 4.0 nM.[27] The imidazole R116010 inhibits ATRA metabolism in intact T47D cells with an IC_{50} value of 8.7 nM.[26] Compound **50** (Chart 1) has also been developed as a competitive inhibitor of CYP26 expressed in HeLa cells, with an IC_{50} value of 14.0 nM.[28] Furthermore, the exceptionally wide range of IC_{50} values (0.000045−36000 nM, spanning 11 orders of magnitude) obtained in this study will enable us to utilize the Catalyst molecular modeling program to create a general pharmacophore model that can differentiate compounds as active or inactive inhibitors of the enzyme complex. These studies, which are currently underway, could lead to the discovery of other potent RAMBAs with nonretinoidal scaffold.

RAMBAs in Cell-Based Assays. To assess the ability of our novel RAMBA to inhibit ATRA metabolism in intact cells, we chose **5**, **6**, **11**, **12**, and **23** to evaluate their inhibitory potencies in two human breast MCF-7 and T47D carcinoma cells. These two breast cancer cell lines are well-known to have inducible ATRA metabolism,[22−26] which closely correlates with the expression levels of CYP26.

Human T47D breast carcinoma cells cultured under control conditions are unable to metabolize ATRA into more polar metabolites (Figure 2A). However, after pretreatment with 1 μM ATRA for 12−15 h, the cells show extensive ATRA metabolism (Figure 2B), converting ATRA into highly polar metabolites (HPM, retention time, R_t = 2−6 min) and prominent metabolites of medium polarity (MMP, R_t = 11−14 min), including 4-oxo- and 4-hydroxy-ATRA. ATRA metabolism is inhibited dose-dependently by **14** (Figure 2C,D). Identical results were also obtained for experiments with MCF7 breast cancer cells and with the other four compounds tested. The IC_{50} values for compounds were determined from dose−response curves and are presented in Table 1. The compounds inhibited intracellular ATRA metabolism to the same extent in both cell lines, with decreasing activity in the order **6** > **11** > **12** > **23** > **5**. Compound **6** was the most active, with an IC_{50} value of 6.3 and 10.9 nM for the T47D and MCF-7 cell lines, respectively. Surprisingly, compound **5**, which was the most potent inhibitor of hamster liver microsomal enzyme, was the least potent, with IC_{50} values of approximately 200 nM in both cell lines. The inhibitory potency of our best RAMBA, **6** (IC_{50} = 6.3 nM), is comparable to the potency of R116010 (IC_{50} = 8.7 nM)[26] in intact human T47D breast cancer cells.

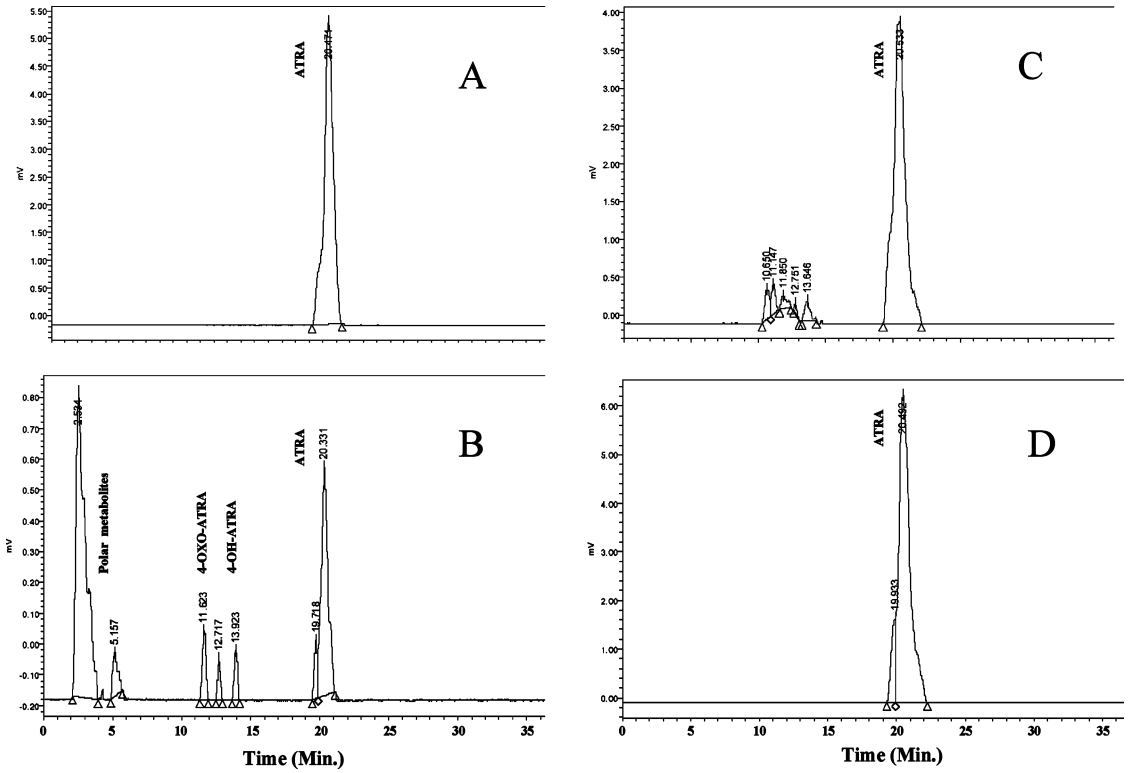

Figure 2. HPLC analysis of [11,12-^{3}H]-ATRA metabolites formed in human T47D breast cancer cells. Human T47D breast cancer cells were cultured under basal conditions (A) or pretreated with 1 μM ATRA (B−D). Thereafter, cell were collected, washed, and incubated with 0.1 μM [11,12-^{3}H]-ATRA, either in the absence (A and B) or in the presence (C and D) of **6** at concentrations of 10 and 100 nM, respectively. The cells and media were extracted and analyzed by reverse phase HPLC as described in the Experimental Section.

Our compounds also inhibited ATRA metabolism of microsomes prepared from T47D cells previously exposed to ATRA in a concentration-dependent manner, with IC_{50} values of 40.0, 2.4, and 5.3 nM for **5**, **6**, and **11**, respectively (Table 1). The inhibition trend of these RAMBAs in microsomes was similar to that in cells, but with 2−5-fold higher potencies. These differences may be due to the different capabilities of the various RAMBAs to penetrate the cell membranes of the T47D breast cancer cells. Similar results have recently been reported for farnesol derivatives that are weak inhibitors of ATRA metabolism in human head and neck squamous cell carcinoma (AMC-HN-6) cells and their microsomal preparations.[40]

Inhibition of ATRA Metabolism by 5 and Its Enantiomers. Because the enantiomers of the 4-azole derivatives may show differences in enzyme inhibitory potencies, we separated the enantiomers of our most potent inhibitor, racemate **5**, to give (4*R*)-(−)-**5** and (4*S*)-(+)-**5** and then tested their abilities to inhibit ATRA metabolism in intact T47D breast cancer cells and in their microsomal preparations. The IC_{50} values are shown in Table 1. Here again, the inhibition trend of the three compounds in microsomes was similar to that in intact cells, but with 5−9-fold higher potency. Surprisingly, the racemate was considerably (up to 28-fold) more potent than the enantiomers, and, quite unexpectedly, there was essentially no difference in activity between the two enantiomers. This lack of stereoselectivity is obviously not due to racemization of the enantiomers in the assay medium, for, if this were the case, then their activities would be the same as that of the racemate. Although the other racemates were not separated into their respective enantiomers and tested for enzyme inhibition, it is likely that they may also behave in a similar fashion. The reason(s) underlying this lack of stereoselectivity is unknown at this time, but might be the consequence of phenomena occurring at the active site of the enzyme. However, it should be stated that there is precedent for this kind of phenomenon with a few examples of enantiopure azole derivatives having the azole moiety directly linked to the stereogenic center.[41]

Overall, these enzyme studies confirm our novel compounds as potent inhibitors of ATRA metabolism not only in liver microsomes but also in ATRA-induced ATRA metabolism in intact cells and their microsomes. Notably, we observed a significant difference between the inhibitory potencies of our compounds toward microsomal enzymes from hamster liver and from T47D and MCF-7 human breast cancer cells. These differences most probably reflect the unique nature of the ATRA-metabolizing CYP(s) present in the two systems. Thus, our potent inhibitors might be superior to other RAMBAs in animal models.

Effects of 6 and 11 on the Antiproliferative Activity of ATRA. The ability of **6** and **11** to enhance the antiproliferative activity of ATRA in MCF-7 breast cancer cells was also studied. MCF-7 cells were continuously incubated with ATRA (0.1 to 10000 nM) alone and in combination with low doses (10 nM each, doses that exhibit low [∼10%] antiproliferative effects, see Figure 3B) of **6** and **11**. ATRA inhibited MCF-7 cell proliferation in a dose-dependent manner (Figure 3A) with an IC_{50} value of 584.50 nM. Both **6** and **11** each in combination with ATRA significantly enhanced the antiproliferativ

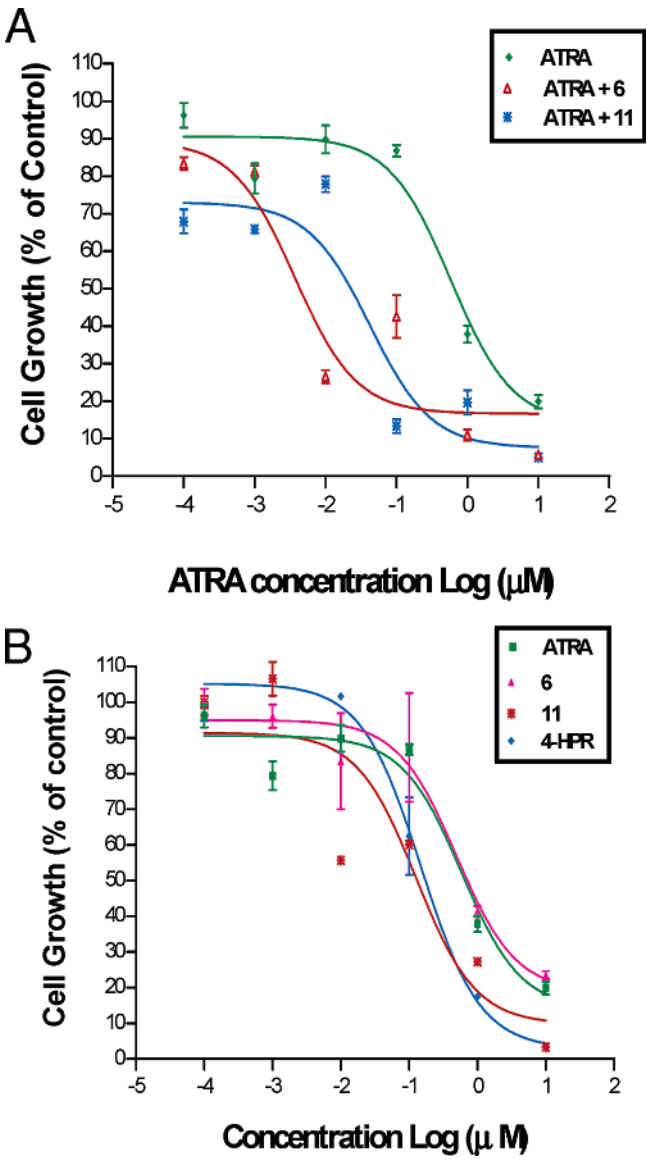

Figure 3. (A) Antiproliferative effects of ATRA alone and ATRA in combination with **6** or **11** at 10 nM each. MCF-7 cell proliferation was measured after 6 days of treatments using a MTT assay as described in the Experimental Section. Results are presented as SEM of three independent experiments. (B) Antiproliferative effects of ATRA, 4-HPR, and RAMBAs **6** and **11**. MCF-7 cell proliferation was measured after 6 days of treatments using a MTT assay as described in the Experimental Section. Results are presented as SEM of three independent experiments.

activity of ATRA, by 159- and 14-fold, respectively (for **6**, IC_{50} from 584.50 to 3.69 nM; and for **11**, IC_{50} from 584.50 to 41.74 nM) (Figure 3A). As expected, concentrations effective in enhancing the biological activity of ATRA are identical to the concentrations required to inhibit ATRA metabolism in intact cells. These results appear to be the most impressive of any RAMBA for which comparable data have been previously described. R116010 (Chart 1), at a concentration 1 μM (*100 times higher than the concentration of* ***6*** *or* ***11***), enhanced the antiproliferative activity of ATRA in human breast T47D cancer cells by only 3-fold.[26] In the same study, liarozole, tested up to a concentration of 10 μM, was unable to enhance the antiproliferative activity of ATRA. Taken together, our results support the hypothesis that our novel RAMBAs are able to enhance the biological activity of ATRA through the inhibition of ATRA metabolism in MCF-7 cells.

Table 3. Inhibitory Concentrations (IC_{50} μM)[a] of RAMBAs and Reference Compounds, ATRA and 4-HPR, in Nuclear Retinoic Acid Receptor (RAR) Binding

	IC_{50} (μM)		
RAMBA[b]	RARα	RARβ	RARγ
6	20	175	45
9	>1000	1000	700
10	410	250	300
13	≫1000	~500	~500
14	20	90	80
21	100	175	65
for comparison:			
ATRA[c]	9	3	10

[a] The IC_{50} values were determined from dose−response curves compiled from at least two independent experiments and represent the compound concentration (nM) required to inhibit cell proliferation by 50%. [b] The other RAMBA (**8**, **11**, **12**, **15**, **22** and **23**) to any of the three RARs at concentrations up to 500 nM. [c] IC_{50} values were taken from Idres et al.[43]

Other Biological Activities. Given the retinoidal nature of our RAMBAs, it seemed logical to investigate their effects on the growth of cancer cells. The antiproliferative effects of ATRA and 4-hydroxyphenyl-retinamide (4-HPR) were also studied for comparison using a MTT assay.[42] Continuous exposure of MCF-7 cells to various doses of the RAMBAs and the two reference compounds for 6 days led to dose-dependent inhibition of cell growth as shown in Figure 3B. The calculated IC_{50} values (defined as the concentration of compounds required to inhibit cell growth by 50%) from these dose−response curves are listed in Table 2. These compounds were also studied in a panel of other human cancer cell lines—breast (T47D and MD-MB-231) and prostate (LNCaP and PC-3)—and their IC_{50} values are also presented in Table 2. The compounds inhibited cell growth to varying degrees, with two breast cancer cells (T47D and MCF-7) exhibiting exquisite sensitivity to most of the RAMBAs. This suggests that the observed

Table 2. Inhibitory Concentrations (IC_{50} μM)[a] of RAMBAs and Reference Compounds, ATRA and 4-HPR, on the Growth of Human Cancer Cell Lines in Vitro

		IC_{50} (μM)						
cell line	tumor type	ATRA	4-HPR	**5**	**6**	**11**	**12**	**13**
MCF-7	breast carcinoma	0.58	0.15	–	0.49	0.13	0.61	–
T47D		0.006	–	–	0.003	0.009	0.57	–
MDA-MB-231		ni	7.7	7.5	ni	ni	6.3	7.0
LNCaP	prostate carcinoma	10.0	7.5	–	10.0	10.0	9.0	–
PC-3		2.0	3.6	–	7.7	5.8	1.5	–

[a] The IC_{50} values were determined from dose−response curves (by a nonlinear regression analysis using GraphPad Prism) compiled from at least two independent experiments and represent the compound concentration (μM) required to inhibit cell proliferation by 50%; ni = no inhibition up to 10 μM; − = not determined.

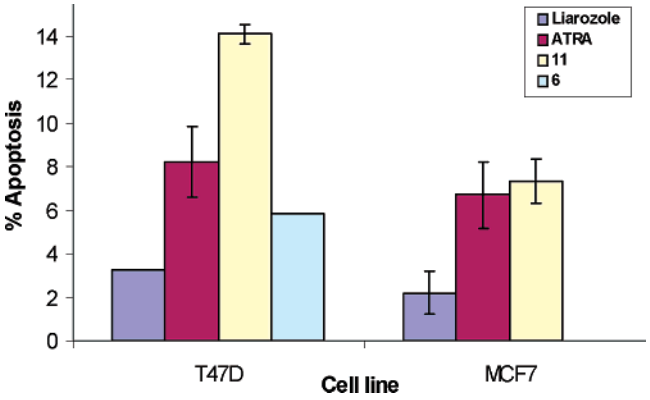

Figure 4. Effects of ATRA, liarozole and RAMBAs **6** and **11** on apoptosis in human breast cancer (T47D and MCF-7) cells. Cells were treated with 1 μM each of ATRA, liarozole, and RAMBAs (**6** and **11**) for 6 days; apoptosis was determined by APO-BRDU (TUNEL assay) and analyzed using flow cytometry.

cancer cell growth inhibition is specific and not due to "general toxicity" of the active RAMBAs. Furthermore, the data suggest that our RAMBAs might also possess retinoidal and/or *4-HPR-like* activities that could strengthen their therapeutic potentials.

The capacity of some RAMBAs to bind to retinoic acid receptors (RARs) was briefly investigated in competitive binding assays using 1 nM [11,12-^{3}H]-ATRA and various concentrations of the RAMBAs ranging from 1 to 1000 nM. The specific binding of ATRA in the absence of RAMBA was set at 100. The IC_{50} values determined from dose−response curves are presented in Table 3, and examples of the competitive binding with **6** and **14** are depicted in Figure B (Supporting Information). The best competitive binders for the three RARα, -β, and -γ were **6** with IC_{50} values of 20, 175, and 45 nM, respectively, followed by **14** (IC_{50} values: 20, 90, and 80 nM) and **21** (IC_{50} values = 100, 175, and 65 nM). These IC_{50} values are ~2-fold (for RARα), 30-fold (for RARβ), and ~4.5-fold (for RARγ) higher than those of ATRA and its natural isomers for binding to RAR receptors.[43] With the exception of **14**, the RAMBAs that do not have the free terminal carboxylic acid moiety did not bind to any of the three RARs in vitro at concentrations up to 500 nM. The low IC_{50} values for **14** were unexpected because of the absence of a terminal free carboxylic acid group in this molecule. However, it is plausible that the terminal triazole group is relatively acidic to interact favorably with RAR active site groups. Collectively, these results suggest that some of our RAMBAs may possess RAR receptor-dependent/independent mechanism of action as well as inhibition of ATRA 4-hydroxylase activity. Studies to assess the transactivation activities of **6**, **14**, and **21** toward RARα, -β, and -γ are planned.

The cellular effects of **6** and **11** were studied briefly in two breast cancer cell lines, MCF-7 and T47D, and one prostate cancer cell line, LNCaP. The effects of **6** and **11** with ATRA as a reference on breast cancer cell apoptosis were monitored using a TUNEL assay to detect intranuclear DNA damage in situ.[44] Figure 4 indicates that both compounds were effective apoptosis inducers, but **11** was more effective. Because of their potent RAMBA activity, these two compounds are expected to be strong enhancers of the proapoptotic action of ATRA. The potential effects of these two compounds on cell differentiation were also briefly studied in LNCaP human prostate cancer cells by assessing the expression of cytokeratin 18 (CK18).[45] Figure 5 shows the results obtained by treating LNCaP cells with ATRA, **6**, and **11** (1 μM each) alone and ATRA in combination with either **6** or **11**. Both compounds induced differentiation and also significantly enhanced ATRA-induced differentiation in this cell line. These results are encouraging, and more detailed cellular experiments are planned. Liarozole, a weak inhibitor of ATRA metabolism, has been shown to effectively enhance the proapoptotic and prodifferentiation activities of ATRA in a variety of in vitro and in vivo

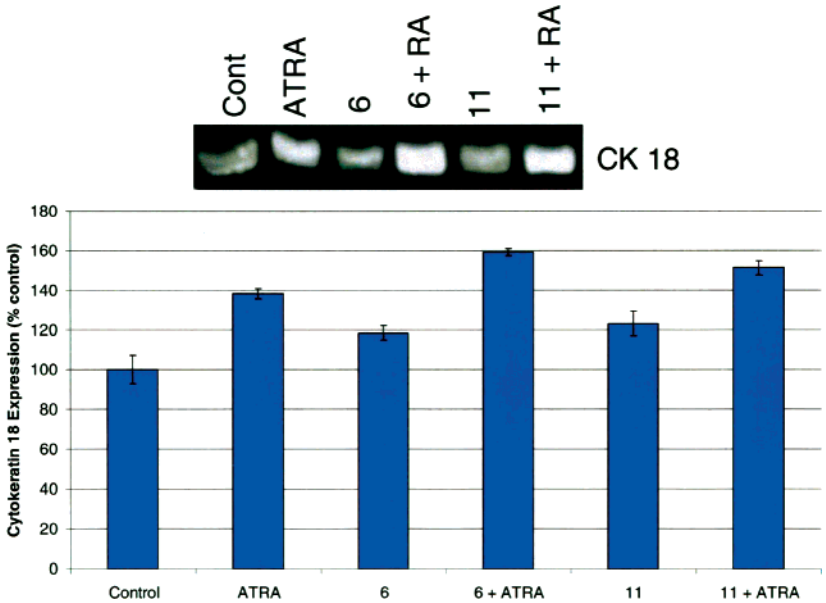

Figure 5. Effects of ATRA and RAMBAs **6** and **11** on levels of cytokeratin 18 (CK18, a differentiation marker) in human prostate LNCaP cells. Cells were incubated with ATRA alone or in combination with **6** or **11** for 6 days. Lysates were subjected to SDS−PAGE and Western blotting. Membranes were probed with CK18 antibody, and the intensities of bands were analyzed by densitometry.

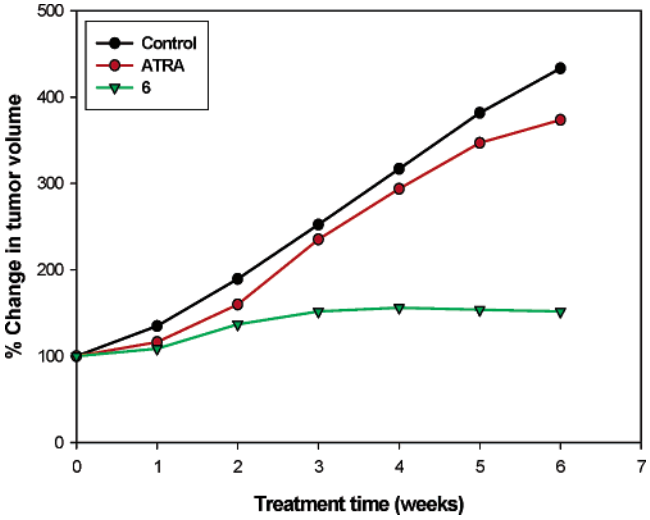

Figure 6. The effects of ATRA and RAMBA **6** (VN/14-1) on the growth of estrogen-dependent human MCF-7 breast tumor in ovariectomized nude mice supplemented with estradiol. Groups of five mice with MCF-7 tumors were treated with the compounds (ATRA and **6**) at 0.033 μmol/kg/day (6 days per week) for 6 weeks. Tumor volumes and body weights were measured weekly, and the percentage change in tumor volume was determined.

models.[5,6,46] Because our RAMBAs are significantly more potent than liarozole, low doses would be required to attain optimal effects and therefore are less likely to produce other unwanted effects.

In Vivo Antitumor Studies. Female ovariectomized nude mice bearing MCF-7 tumor xenografts (approximately 300 mm^3) were treated once daily with 0.033 mmol/kg each of **6** (VN/14-1) or ATRA for six weeks. As shown in Figure 6, VN/14-1 caused a significant reduction of 85.2% in the mean final tumor volume compared with vehicle-treated control animals (p = 0.022). Interestingly, the two tumors that were present in one of the five VN/14-1-treated mice were not palpable (from week 4 to 6), indicating a complete regression of these tumors after drug treatment. VN/14-1 did not alter body weights of mice, and other signs of retinoid clinical toxicity were not observed. In contrast, ATRA did not exhibit significant tumor growth inhibition in this xenograft model (Figure 6). It was recently reported[26] that the growth of murine estrogen-independent TA3-Ha mammary tumors was significantly inhibited by R116010. In addition, ATRA also exhibited strong antitumor efficacy, albeit at a higher dose. This study demonstrates the antitumor efficacy of R116010 in an estrogen-independent model of unestablished tumors. However, it is not known whether they are effective in estrogen-dependent models. Given that VN/14-1 exhibited potent antitumor efficacy in the estrogen-dependent mammary carcinoma model and also on well-established tumors of about 300 mm^3, it seems probable that VN/14-1 may be a more effective anticancer agent.

Conclusions

We have shown that C-4 azolyl RAMBAs, rationally designed analogues of retinoic acid, potently inhibit ATRA metabolism catalyzed by liver microsomes and CYP26 in intact breast cancer cells, but in contrast to other RAMBAs, they are endowed with multiple desirable anticancer activities. Because of their unique characteristics, these novel compounds may have anticancer activity not possible with other RAMBAs. The lead compound **6** (VN/14-1) inhibits the growth of human breast MCF-7 tumors in nude mice. In this model, VN/14-1 showed superior antitumor activity to ATRA. This and related RAMBAs warrant further evaluation as potential therapeutic agents in breast cancer as well as in other varieties of cancers.

Experimental Section

Chemistry. General procedures and techniques were identical with those previously reported.[28] ^{1}H NMR spectra were recorded in $CDCl_3$ at 300, 500, or 600 MHz with Me_4Si as an internal standard. ^{13}C NMR spectra were performed in $CDCl_3$ and obtained using a Varian Inova 500 MHz spectrometer operating at 125 MHz or Bruker Advance DMX600 spectrometer operating at 150 MHz. High-resolution mass spectra (HRMS) were determined on a Karatos-Aspect Systems instrument, EI mode. Low-resolution mass spectra (LRMS) were determined on a Finnegan LCR-MS. Optical rotations were measured at the sodium line using a Perkin-Elmer 141 polarimeter and are the average of seven values. Retinoids (*all-trans*-retinoic acid and *N*-(4-hydroxyphenyl)retinamide (4-HPR) were purchased from Sigma-Aldrich, St. Louis, MO, and from LKT Laboratories, Inc., St. Paul, MN. Liarozole was a gift from Dr. Marcel Janssen of Johnson and Johnson Pharmaceutical Research and Development, Beerse, Belgium.

Although the retinoidal intermediates and final products appeared to be relatively stable to light, precautions were taken to minimize exposure to any light source and to the atmosphere. Thus, all operations were performed in dim light, with reaction vessels wrapped with aluminum foil. All compounds were stored in an atmosphere of argon and in the cold (−20 or −80 °C) and dark without significant decomposition.

4-(±)-(1*H*-Imidazol-1-yl)-(*E*)-methylretinoate (5)[47] and Resolution to (4*R*)-(−)-5 and (4*S*)-(+)-5. To a solution of 4-hydroxy-(*E*)-methylretinoate (**4**, 3.0 g, 9.09 mmol) in dry CH_3CN (50 mL) was added 1,1′-carbonyldiimidazole (CDI) (1.95 g, 12.0 mmol, 1.3 equiv), and the reaction mixture was stirred at room temperature for 30 min, at which time the reaction was complete as determined by TLC. Following addition of cold water (100 mL), the reaction mixture was extracted with 10% MeOH in $CHCl_3$ (50 mL × 3). The combined extract was washed with brine, dried, and concentrated to give a yellow viscous oil. This crude product was dissolved in 10 mL of CH_2Cl_2/EtOAc/Et_3N (7:3:0.3, v/v/v) and filtered through a 3 in. column of silica gel (70−230 mesh). The column was washed with the same solvent, and four fractions of 50, 100, 150, and 150 mL were collected. Pure product was present in the third fraction, which was concentrated to give a viscous yellow oil that crystallized on storage at −20 °C after approximately 12 h. Following trituration in 10 mL of EtOAc/pet ether (9:1, v/v), the yellow crystals were filtered off and dried under vacuum to give the title compound **5** (3.4 gm, 89.5%): mp 118−120 °C. ^{1}H NMR (300 MHz, $CDCl_3$): δ 1.09 (s, 3H, 16-CH_3), 1.12 (s, 3H, 17-CH_3), 1.60 (s, 3H, 18-CH_3), 2.02 (s, 3H, 19-CH_3), 2.36 (s, 3H, 20-CH_3), 3.72 (s, 3H, 15-OCH_3), 4.53 (s, 1H, 4-H), 5.80 (s, 1H, 14-H), 6.25 (m, 4H, 7-, 8-, 10- and 12-Hs), 6.91 (s, 1H, 4^1-H), 6.98 (t, 1H, J = 14.7 Hz, 11-H), 7.07 (s, 1H, 5^1-H), 7.50 (s, 1H, 2^1-H). ^{13}C NMR (150 MHz, $CDCl_3$): δ 167.5 (C-15), 152.6 (C-13), 144.9 (C-9), 139.1 (C-8), 138.5 (C-6), 136.8 (C-2^1), 136.1 (C-12), 131.1 (C-11), 130.6 (C-10), 129.1 (C-7), 126.7 (C-5), 118.7 (C-14), 125.0 (C-4^1), 118.2 (C-5^1), 58.1 (C-4), 52.0 (15-OCH_3), 34.7 (C-2), 34.6 (C-1), 29.0 and 28.2 (C-16 and C-17), 27.8 (C-18), 18.9 (C-3), 13.8 (C-20), and 12.9 (C-19). HRMS: calcd 380.2464 ($C_{24}H_{32}O_2N_2$), found 380.2451.

Resolution of (±)-5. A racemic sample of **5** (40 mg) was dissolved in 8 mL of *n*-hexane/isopropyl alcohol, 90:10; v/v. This solution (100 μL/run) was charged to the chiral column (Chiralpak AD, 10 μm, 4.6 × 250 mm) and eluted with

n-hexane−isopropyl alcohol (95:5, v/v) at a flow rate of 0.75 mL/min, using a photodiode array (PDA) detector. The retention times for the first (A) and second (B) peaks were 25.19 and 28.89 min, respectively. Eluents of each peak were carefully collected manually. The fractions were checked for enantiomeric purity, using conditions essentially similar to those described above, but with a flow rate of 1.5 mL/min, with retention times of peaks A and B of 18.42 and 21.42 min, respectively. The pure fractions for each peak were combined and evaporated to dryness under vacuum to give 12 mg of peak A and 16 mg of peak B. The chemical structures were confirmed by ^{1}H NMR spectrum and identical as expected. Optical rotations were measured at the sodium line using a Perkin-Elmer 141 polarimeter and are averages of seven values. For peak A, (4*R*)-(−)-**5**, $[\alpha]^{24}_D = -25.8°$ ($c = 0.46$, $CHCl_3$), and for peak B, (4*S*)-(+)-**5**, $[\alpha]^{24}_D = +25.3°$ ($c = 0.46$, $CHCl_3$), respectively.

4-(±)-(1*H*-Imidazol-1-yl)-(*E*)-retinoic Acid (6). To a solution of **5** (2.5 g, 6.57 mmol) in methanol (25 mL) was added 2 N KOH (40 mL, solution in MeOH/H_2O, 9:1, v/v), and the mixture was stirred under an Ar atmosphere at reflux for 2 h, then concentrated to 1/5 the original volume, cooled, poured into cold water, neutralized (to pH ∼ 7) with 6 N HCl, and extracted with 5% MeOH in EtOAc (50 mL × 3). The combined extract was washed with brine (×3), dried (Na_2SO_4), and concentrated. Trituration in petroleum ether gave pure **6** (2.2 g, 91%). Details of most physical and spectroscopic data have been previously reported.[28] Hitherto unreported ^{13}C NMR data are provided below. ^{13}C NMR (150 MHz, $CDCl_3$ + DMSO-d_6): δ 170.1 (C-15), 155.2 (C-13), 147.5 (C-9), 141.7 (C-8), 141.1 (C-6), 139.4 (C-2^1), 138.7 (C-12), 133.6 (C-11), 133.2 (C-10), 131.7 (C-7), 129.3 (C-5), 121.3 (C-14), 127.6 (C-4^1), 120.8 (C-5^1), 60.7 (C-4), 37.3 (C-2), 37.2 (C-1), 31.6 and 30.8 (C-16 and C-17), 30.4 (C-18), 21.5 (C-3), 16.4 (C-20), and 15.5 (C-19).

4-(±)-(1*H*-1,2,4-Triazol-1-yl)-(*E*)-methylretinoate (7) and 4-(±)-(4*H*-1,2,4-Triazol-4-yl)-(*E*)-methylretinoate (8).[47] To a solution of **4** (1.0 gm, 3.0285 mmol) in dry CH_3CN (15 mL) was added 1,1′-carbonyldi(1,2,4-triazole) (CDT) (693 mg, 4.22 mmol), and the reaction mixture was stirred at room temperature for 30 min, was poured into cold water (50 mL), and then was extracted with 10% MeOH in EtOAc (50 mL × 3). The combined extract was washed with brine (×2), dried, and evaporated to give a yellow viscous oil, which was purified by FCC [silica gel, CH_2Cl_2/EtOH, (35:1, v/v)] to give first **7** (705 mg, 61.1%): mp 105−108 °C. NMR (300 MHz, $CDCl_3$): δ 1.10 (s, 3H, 16-CH_3), 1.13 (s, 3H, 17-CH_3), 1.63 (s, 3H, 18-CH_3), 2.02 (s, 3H, 19-CH_3), 2.36 (s, 3H, 20-CH_3), 3.72 (s, 3H, 15-OCH_3), 4.82 (s, 1H, 4-H), 5.80 (s, 1H, 14-H), 6.30 (m, 4H, 7-, 8-, 10- and 12-Hs), 6.99 (t, 1H, $J = 14.7$ Hz, 11-H), 7.99 (s, 1H, 3^1-H), 8.02 (s, 1H, 5^1-H). ^{13}C NMR (150 MHz, $CDCl_3$): δ 167.4 (C-15), 152.6 (C-13), 151.9 (C-3^1), 142.5 (C-5^1), 146.0 (C-9), 139.2 (C-8), 138.4 (C-6), 136.3 (C-12), 131.1 (C-11), 130.5 (C-10), 126.4 (C-7), 123.6 (C-5), 118.5 (C-14), 61.1 (C-4), 51.0 (15-OCH_3), 34.8 (C-2), 34.0 (C-1), 29.1 and 28.2 (C-16 and C-17), 26.3 (C-18), 19.0 (C-3), 13.8 (C-20), and 12.9 (C-19). HRMS: calcd 381.2416 ($C_{23}H_{31}O_2N_3$), found 381.2442.

Further elution with CH_2Cl_2/EtOH, 20:1, v/v, afforded **8** (390 mg, 33.8%): mp 62−65 °C. NMR (300 MHz, $CDCl_3$): δ 1.10 (s, 3H, 16-CH_3), 1.13 (s, 3H, 17-CH_3), 1.64 (s, 3H, 18-CH_3), 2.02 (s, 3H, 19-CH_3), 2.36 (s, 3H, 20-CH_3), 3.72 (s, 3H, 15-OCH_3), 4.64 (s, 1H, 4-H), 5.81 (s, 1H, 14-H), 6.25 (m, 4H, 7-, 8-, 10- and 12-Hs), 6.98 (t, 1H, $J = 14.7$ Hz, 11-H), 8.15 (s, 1H, 3^1- and 5^1-H). ^{13}C NMR (150 MHz, $CDCl_3$): δ 167.4(C-15), 152.5 (C-13), 146.5 (C-9), 142.3 (C-2^1 and C-3^1), 139.6 (C-8), 137.5 (C-6), 136.5 (C-12), 131.4 (C-11), 130.4 (C-10), 125.9 (C-7), 123.1 (C-5), 118.9 (C-14), 57.0 (C-4), 51.0 (15-OCH_3), 34.7 (C-2), 33.8 (C-1), 29.2 and 28.2 (C-16 and C-17), 27.5 (C-18), 19.1 (C-3), 13.8 (C-20), and 12.9 (C-19). HRMS: calcd 381.2416 ($C_{23}H_{31}O_2N_3$), found 381.2423.

4-(±)-(1*H*-1,2,4-Triazol-1-yl)-(*E*)-retinoic Acid (9). The method followed that described for **6** but used **7** (500 mg, 1.31 mmol). Trituration in petroleum ether gave pure **9** (409 mg, 85%). Details of most physical and spectroscopic data have been previously reported.[28] Hitherto unreported ^{13}C NMR data are provided below. ^{13}C NMR (150 MHz, $CDCl_3$ + DMSO-d_6): δ 167.4 (C-15), 152.6 (C-13), 151.9 (C-3^1), 142.5 (C-5^1), 146.0 (C-9), 139.2 (C-8), 138.4 (C-6), 136.3 (C-12), 131.1 (C-11), 130.5 (C-10), 126.4 (C-7), 123.6 (C-5), 118.5 (C-14), 61.1 (C-4), 34.8 (C-2), 34.0 (C-1), 29.1 and 28.2 (C-16 and C-17), 26.3 (C-18), 19.0 (C-3), 13.8 (C-20), and 12.9 (C-19).

4-(±)-(1*H*-1,2,4-Triazol-4-yl)-(*E*)-retinoic Acid (10). The method followed that described for **6** but used **8** (250 mg, 0.656 mmol). Trituration in petroleum ether gave pure **10** (193 mg, 80%). Details of most physical and spectroscopic data have been previously reported.[28] Hitherto unreported ^{13}C NMR data are provided below. ^{13}C NMR (150 MHz, $CDCl_3$ + DMSO-d_6): δ 168.4 (C-15), 152.5 (C-13), 146.5 (C-9), 142.3 (C-2^1 and C-3^1), 139.6 (C-8), 137.5 (C-6), 136.5 (C-12), 131.4 (C-11), 130.4 (C-10), 125.9 (C-7), 123.1 (C-5), 118.9 (C-14), 57.0 (C-4), 34.7 (C-2), 33.8 (C-1), 29.2 and 28.2 (C-16 and C-17), 27.5 (C-18), 19.1 (C-3), 13.8 (C-20), and 12.9 (C-19).

4-(±)-(1*H*-Imidazol-1-yl)-*N*-(imidazolyl)-(*E*)-retinamide (11). To a suspension of **6** (800 mg, 2.18 mmol) in dry CH_3CN (20 mL) was added CDI (460.6 mg, 2.84 mmol), and the mixture was stirred at room temperature for 1 h, poured into cold water (100 mL), and then extracted with 5% MeOH in ether (50 mL × 3). The combined extract was washed with brine, dried (Na_2SO_4), and concentrated to give an oily dark red product. This crude product was dissolved in a mixture of CH_2Cl_2/MeOH/Et_3N (15:1:0.2, v/v/v) and filtered through a 3 in. silica gel column that was eluted with the same solvent mixture. The fraction that contained pure **11** (as determined by TLC) was concentrated, dried under vacuum, and stored at −20 °C for approximately 12 h to give the desired **11** (850 mg, 95%): mp 82−85 °C. ^{1}H NMR (500 MHz, $CDCl_3$): δ 1.15 (s, 3H, 16-CH_3), 1.18 (s, 3H, 17-CH_3), 1.65 (s, 3H, 18-CH_3), 2.11 (s, 3H, 19-CH_3), 2.55 (s, 3H, 20-CH_3), 4.59 (t, 1H, $J = 5$ Hz, 4-H), 6.26 (d, 1H, $J = 26.5$ Hz, 8-H), 6.28 (s, 1H, 14-H), 6.46 (m, 3H, 7-, 10-H and 12-Hs), 6.96 (s, 1H, 4^1-H), 7.12 (s, 1H, 5^1-H), 7.14 (s, 1H, 4^{11}-H), 7.25 (dd, 1H, $J_1 = J_2 = 11$ Hz, 11-H), 7.55 (s, 1H, 2^1-H), 7.58 (s, 1H, 5^{11}-H), 8.24 (s, 1H, 2^{11}-H). ^{13}C NMR (125 MHz, $CDCl_3$): δ 162.0 (C-15), 159.0 (C-13), 145.1 (C-9), 141.0 (C-2^1), 139.1 (C-8), 136.9 (C-6 and C-2^1), 136.3 (C-12 and C-2^{11}), 135.4 (C-10), 133.8 (C-11), 130.7 (C-7), 131.0 (C-5), 129.1 (C-4^1), 118.5 (C-14), 116.5 (C-5^{11}), 115.9 (C-5^1), 58.4 (C-4), 34.8 (C-2), 29.3 (C-1), 28.3 (C-17), 28.0 (C− 16), 22.8 (C-18), 19.1 (C-3), 15.3 (C-20), and 13.3 (C-19). HRMS: calcd 416.2576 ($C_{26}H_{32}ON_4$), found 416.2354.

4-(±)-(1*H*-Imidazol-1-yl)-*N*-(4-hydroxyphenyl)-(*E*)-retinamide (12). Compound **6** (740 mg, 2.02 mmol), *p*-aminophenol (264.6 mg, 2.424 mmol), and 1-hydroxybenzotriazole (HOBT) (327.6 mg, 2.424 mmol) were dissolved in dry DMF (5 mL) and cooled to 0 °C. Dicyclohexylcarbodiimide (DCC), (500.2 mg, 2.424 mmol) was added, and the mixture was allowed to warm to room temperature. After stirring for approximately 20 h, the precipitated dicyclohexyl urea was filtered off and washed with 5% MeOH in EtOAc. The filtrate was washed with water, brine, dried (Na_2SO_4), and concentrated to give crude product (1.2 g), which was purified by FCC (silica gel, CH_2Cl_2/MeOH/Et_3N, 15:1:0.2, v/v/v) to give **12** (510 mg, 55%): mp 125−129 °C. ^{1}H NMR (500 MHz, $CDCl_3$): δ 1.09 (s, 3H, 16-CH_3), 1.10 (s, 3H, 17-CH_3), 1.59 (s, 3H, 18-CH_3), 1.99 (s, 3H, 19-CH_3), 2.38 (s, 3H, 20-CH_3), 4.53 (t, 1H, $J = 5$ Hz, 4-H), 5.89 (s, 1H, 14-H), 6.20 (m, 4H, 7-, 8-, 10-H and 12-Hs), 6.81 (d, 2H, $J = 9$ Hz, aromatic Hs), 6.90 (dd, 1H, $J_1 = J_2 = 11$ Hz, 11-H), 6.93 (s, 1H, 4^1-H), 7.09 (s, 1H, 5^1-H), 7.37 (d, 2H, $J = 8.5$ Hz, aromatic Hs), 7.54 (s, 1H, 2^1-H), 7.80 (s, 1H, NH). ^{13}C NMR (150 MHz, $CDCl_3$): δ 165.2 (C-15), 154.0 (C-13), 149.3 (C-9), 145.4 (C-1^{11} and 4^{11}), 139.5 (C-8), 137.7 (C-6), 137.6 (C-2^1), 136.9 (C-12), 134.4 (C-11), 131.4 (C-10), 130.4 (C-7), 126.1 (C-5), 126.1 (C-4^1), 124.5 (C-5^1), 122.0 (2 aromatic Cs), 115.9 (2 aromatic Cs), 118.6 (C-14), 58.5 (C-4), 34.7 (C-2), 34.6 (C-1), 29.2 and 28.2 (C-16 and C-17), 27.8 (C-18), 19.0 (C-3), 12.9 (C-20), and 13.7 (C-19). HRMS: calcd 457.2729 ($C_{29}H_{35}O_2N_3$), found 457.2634.

4-Hydroxyimino-(*E*)-methylretinoate (15). A solution of ketone **3** (400 mg, 1.2192 mmol) in ethanol (8 mL) was treated with a solution of hydroxylamine hydrochloride (184 mg, 2.65

mmol) and anhydrous sodium acetate (138 mg, 1.68 mmol) in 50% aqueous ethanol (12 mL), and the resulting mixture was stirred at room temperature for 24 h. The solvent was removed under reduced pressure at 35 °C, and the residue was diluted with cold water. The resulting yellow precipitate was filtered and dried under vacuum to afford the oxime **15** (339 mg, 85%): mp 172−174 °C. ^{1}H NMR ($CDCl_3$): δ 1.14 (s, 6H, 16- and 17-CH_3), 1.90 (s, 3H, 18-CH_3), 2.07 (s, 3H, 19-CH_3), 2.41 (s, 3H, 20-CH_3), 2.74 (t, 2H, J = 6.5 Hz, 3-CH_2), 3.76 (s, 3H, 15-OCH_3), 5.85 (s, 1H, 14-H), 6.36 (m, 4H, 7-, 8-, 10, and 12-Hs), 7.04 (dd, 1H, $J_1 = J_2$ = 11.5 Hz, 11-H). ^{13}C NMR (125 MHz, $CDCl_3$): δ 167.7 (C-15), 158.0 (C-4), 152.0 (C-13), 149.7 (C-9), 139.4 (C-8), 138.8 (C-12), 136.6 (C-11), 131.5 (C-10), 130.9 (C-7), 127.2 (C-6), 125.2 (C-5), 118.9 (C-14), 51.2 (15-OCH_3), 36.2 (C-2), 35.2 (C-1), 27.8 (C-16 and C-17), 19.6 (C-18), 15.2 (C-3), 14.0 (C-20), and 13.1 (C-19). ESI-MS: m/z 343.2 (M^+).

4-(±)-Hydroxy-(13*Z*)-methylretinoate (19). The method followed that described for **4** (Supporting Information) but used the 13-*cis*-**16** (5.0 gm, 16.65 mmol) via the corresponding methyl ester **17** and the 4 keto ester **18**. Chromatography FCC [silica gel, CH_2Cl_2/EtOH, (75:1, v/v)] afforded pure 4-hydroxy-(13*Z*)-methylretinoate **19** (1.5 g, 35% from 16) as a yellow semisolid. ^{1}H NMR (300 MHz, $CDCl_3$): δ 1.02 (s, 3H, 16-CH_3), 1.05 (s, 3H, 17-CH_3), 1.84 (s, 3H, 18-CH_3), 1.99 (s, 3H, 19-CH_3), 2.08 (s, 3H, 20-CH_3), 3.71 (s, 3H, OCH_3), 4.01 (s, 1H, 4-H), 5.66 (s, 1H, 14-H), 6.27 (m, 3H, 7-, 8- and 10-Hs), 6.97 (t, 1H, J = 12.6 Hz, 11-H), 7.85 (d, 1H, J = 15 Hz, 12-H). ESI-MS: m/z 330.1 (M^+).

4-(±)-(1*H*-Imidazol-1-yl)-(13*Z*)-methylretinoate (20). The method followed that described for **5** but used **19** (1.3 g, 3.94 mmol). The crude product was dissolved in 10 mL of CH_2Cl_2/EtOAc/Et_3N (7:3:0.3, v/v/v) and filtered through a 3 in. column of silica gel (70−230 mesh). The column was washed with the same solvent, and four fractions of 50, 100, 150, and 150 mL were collected. Pure product was present in the third fraction, which was concentrated to give a viscous yellow oil that crystallized on storage at −20 °C after approximately 12 h. Following trituration in 10 mL of EtOAc/petroleum ether (9:1, v/v), the yellow crystals were filtered off and dried under vacuum to give the title compound **20** (1.1 g, 89.5%) as a yellow solid. ^{1}H NMR (300 MHz, $CDCl_3$): δ 1.08 (s, 3H, 16-CH_3), 1.13 (s, 3H, 17-CH_3), 1.60 (s, 3H, 18-CH_3), 2.01 (s, 3H, 19-CH_3), 2.08 (s, 3H, 20-CH_3), 3.71 (s, 3H, OCH_3), 4.53 (s, 1H, 4-H), 5.67 (s, 1H, 14-H), 6.25 (m, 3H, 7-, 8- and 10-Hs), 6.91 (s, 1H, 4^1-H), 6.96 (t, 1H, J = 12 Hz, 11-H), 7.07 (s, 1H, 5^1-H), 7.50 (s, 1H, 2^1-H), 7.80 (d, 1H, J = 14.7 Hz, 12-H). HRMS: calcd 380.2464 ($C_{24}H_{32}O_2N_2$), found 380.2458.

4-(±)-(1*H*-Imidazol-1-yl)-(13*Z*)-retinoic Acid (21). The method followed that described for **6** but used **20** (1.1 g, 2.89 mmol). Following workup of reaction as described for **6**, the combined extract was concentrated to approximately 20 mL and then diluted with petroleum ether. After standing overnight at −20 °C, the yellow crystals were filtered off and dried under vacuum to afford pure **21** (700 mg, 73%): mp 127−130 °C. ^{1}H NMR (500 MHz, $CDCl_3$) δ 1.10 (s, 3H, 16-CH_3), 1.12 (s, 3H, 17-CH_3), 1.58 (s, 3H, 18-CH_3), 2.0 (s, 3H, 19-CH_3), 2.08 (s, 3H, 20-CH_3), 4.58 (t, 1H, J = 5.5 Hz, 4-H), 5.74 (s, 1H, 14-H), 6.24 (m, 3H, 7-, 8-, and 10-Hs), 6.92 (s, 1H, 5^1-H), 6.94 (dd, 1H, $J_1 = J_2$ = 11 Hz, 11-H), 7.17 (s, 1H, 4^1-H), 7.76 (s, 1H, 2^1-H), 7.86 (d, 1H, J = 15 Hz, 12-H). ^{13}C NMR (125 MHz, $CDCl_3$ + DMSO-d_6): δ 170.1 (C-15), 150.6 (C-13), 145.9 (C-9), 139.9 (C-6 and C-8), 138.3 (C-2^1), 132.5 (C-12), 132.5 (C-11), 131.3 (C-7 and C-10), 126. 1(C-4^1 and C-5), 124.5 (C-5^1), 118.8 (C-14), 59.0 (C-4), 34.9 (C-2), 29.3 (C-1), 28.3 (C-16), 28.1 (C-17), 21.2 (C-18), 19.1 (C-3), 14.3 (C-20), and 13.0 (C-19). HRMS: calcd 366.3061 ($C_{24}H_{30}O_2N_2$), found 366.3045.

4-(±)-(1*H*-Imidazol-1-yl)-*N*-(imidazolyl)-(13*Z*)-retinamide (22). The method followed that described for **11** but used **21** (307 mg, 0.84 mmol). Purification of the crude product by FCC [CH_2Cl_2/MeOH/Et_3N (15:1:0.2)] afforded the title compound **22** (279 mg, 80%), a yellow semisolid. NMR (500 MHz, $CDCl_3$): δ 1.12 (s, 3H, 16-CH_3), 1.17 (s, 3H, 17-CH_3), 1.63 (s, 3H, 18-CH_3), 2.09 (s, 3H, 19-CH_3), 2.28 (s, 3H, 20-CH_3), 4.58 (t, 1H, J = 4.5 Hz, 4-H), 6.32 (m, 3H, 7-, 10-H, and 14-Hs), 6.94 (s, 1H, 4^1-H), 7.10 (s, 1H, 5^1-H), 7.13 (s, 1H, 4^{11}-H), 7.22 (dd, 1H, $J_1 = J_2$ = 11 Hz, 11-H), 7.53 (s, 1H, 2^1-H), 7.56 (s, 1H, 5^{11}-H), 7.83 (d, 1H, J = 15.5 Hz, 12-H), 8.23 (s, 1H, 2^{11}-H). ^{13}C NMR (125 MHz, $CDCl_3$): δ 161.1 (C-15), 157.1.0 (C-13), 144.9 (C-9), 141.1 (C-2^1), 139.1 (C-8), 136.8 (C-6), 136.3 (C-2^1), 135.2 (C-12), 131.5 (C-2^{11}), 130.7 (C-4^1), 130.1 (C-11), 129.0 (C-7), 128.0 (C-5), 125.4 (C-4^{11}), 118.3 (C-14), 116.4 (C-5^{11}), 113.8 (C-5^1), 58.2 (C-4), 34.8 (C-2), 34.7 (C-1), 29.1 (C-17), 28.2 (C− 16), 27.9 (C-18), 21.7 (C-3), 18.9 (C-20), and 13.1 (C-19). HRMS: calcd 416.2576 ($C_{26}H_{32}ON_4$), found 416.2526.

4-(±)-(1*H*-Imidazol-1-yl)-*N*-(4-hydroxyphenyl)-(13*Z*)-retinamide (23). The method followed that described for **12** but used **21** (200 mg, 0.55 mmol). Purification of the crude product by FCC [CH_2Cl_2/MeOH/Et_3N (15:1:0.2)] afforded the title compound **23** (150 mg, 60%): mp 116−120 °C. NMR (500 MHz, $CDCl_3$): δ 1.06 (s, 3H, 16-CH_3), 1.07 (s, 3H, 17-CH_3), 1.10 (s, 3H, 18-CH_3), 1.58 (s, 3H, 19-CH_3), 2.00 (s, 3H, 20-CH_3), 4.53 (t, 1H, J = 4 Hz, 4-H), 5.72 (s, 1H, 14-H), 6.15 (m, 3H, 7-, 8-, and 10-Hs), 6.81 (d, 2H, J = 9 Hz, aromatic Hs), 6.85 (dd, 1H, $J_1 = J_2$ = 11 Hz, 11-H), 6.93 (s, 1H, 4^1-H), 7.09 (s, 1H, 5^1-H), 7.38 (d, 2H, J = 8 Hz, aromatic Hs), 7.53 (s, 1H, 2^1-H), 7.79 (s, 1H, NH), 7.91 (d, 1H, J = 15.5 Hz, 12-H). ^{13}C NMR (150 MHz, $CDCl_3$): δ 165.2 (C-15), 154.0 (C-13), 149.3 (C-9), 145.4 (C-1^{11} and 4^{11}), 139.7 (C-8), 137.6 (C-6), 137.6 (C-2^1), 136.5 (C-12), 132.4 (C-11), 131.0 (C-10), 130.5 (C-7), 128.4 (C-5), 125.7 (C-4^1), 124.5 (C-5^1), 122.0 (2 aromatic Cs), 118.6 (C-14), 116.0 (2 aromatic Cs), 58.3 (C-4), 34.5 (C-2), 29.1 (C-1), 28.2 (C-16), 27.8 (C-17), 20.9 (C-18), 19.0 (C-3), 12.8 (C-20), and 11.1 (C-19). HRMS: calcd 457.2729 ($C_{29}H_{35}O_2N_3$), found 457.2634.

Enzyme Preparations and Assay Procedures for ATRA Metabolism. Preparation of Microsomes. Microsomes were prepared from the livers of male Syrian golden hamsters and also from human breast cancer cells (MCF-7 and T47D) pretreated with 1 μM ATRA as described by Van Wauwe et al.[39] and Stoppie et al.,[27] respectively. Protein concentrations were determined with a Bio-Rad protein assay kit, obtained from Bio-Rad Laboratories. They were stored at −80 °C.

ATRA Metabolism Assay. We assessed ATRA hydroxylase activity in incubations containing liver or cancer cell microsomes and the inhibitors by measuring the radiolabed polar metabolites produced from [11,12-^{3}H]-ATRA as we have previously described.[30]

All enzymatic studies were performed in 0.1 M phosphate buffer, pH 7.4, at a final incubation volume of 0.40 mL. The incubation mixture contained 100 μL of microsomes (500 μg/mL dissolved in buffer); 100 μL of NADPH (20 mM dissolved in dH_2O); 40 μL of inhibitor (dissolved in DMSO); and 140 μL of assay buffer [0.01 M $MgCl_2$ and 0.02 (w/v) bovine serum albumin (BSA) in phosphate buffer solution]. After a 3 min preincubation at 37 °C, the reaction was initiated by the addition of 20 μL of [11,12-^{3}H]-ATRA (20 μCi/mL) and the incubation was carried out for 30 min under oxygen with shaking in a water bath at 37 °C. The reaction was terminated by the addition of 100 μL of formic acid. The retinoid products were extracted (2×) with 1 mL of ethyl acetate containing 10% methanol and 0.05% butylated hydroxyanisole (BHA). The organic and aqueous phases are separated by centrifugation at 3000*g* for 10 min at 4 °C. The organic phase, containing the retinoids, was dried with a stream of argon and dissolved in 100 μL of methanol for HPLC analysis.

HPLC Analysis. Chromatographic separations and quantification of the retinoids were achieved by a reverse phase HPLC method on a Waters Novapak C_{18} column (3.9 × 300 nm) protected by a Waters guard cartridge packed with pellicular C_{18} as previously described.[30] The HPLC system used in this study consisted of Waters solvent delivery system, Waters controller (Milford, MA), coupled to a Waters 717^{plus} autosampler and a Waters radiomatic detector. Analysis was performed at ambient temperature, and data acquisition and management was achieved with a Waters millennium chromatography manager. On the basis of our procedure,[30] the retinoids (10 μL) were analyzed on a 10 μm C_{18} Bondapak

column eluted with a multilinear gradient solvent system: MeOH−H_2O (60:40) containing 20 mM ammonium acetate (100% → 0%) at 0.8 mL/min for 20 min and MeOH (0% → 100%) at 1 mL/min for the remaining 10 min, during which time the retinoids were eluted with 100% MeOH. Radioactivity was measured by a radiomatic detector. Percent metabolism was obtained by dividing the areas under the curve (AUC) of the metabolite peaks by the AUC of all peaks. IC_{50} values were determined as the concentration of RAMBA that yielded 50% metabolism.

***K*i Assay Procedure.** This procedure is essentially similar to that employed in the dose−response curve IC_{50}-determination assay, except that the substrate concentration was varied between 2 and 10 nM using 250 μg of protein to ensure a constant initial velocity, even at the lowest substrate concentration. Control samples with no inhibitors were also incubated simultaneously. Each inhibitor was examined at one concentration (10 pM, 0.1 nM, 10 pM, 1 nM, 10 nM, and 1 nM for **5**, **6**, **11**, **12**, **21**, and **23**, respectively). Data from the various assays were used to obtain Lineweaver−Burk plots (e.g. Figure 2). From these plots, K_i values for the RAMBA and the K_m for ATRA (substrate) were determined (Table 1).

Cell Culture. Human mammary-carcinoma cell lines MCF-7 and T47D (both ER +ve) and MDA-MB-231 (ER -ve) as well as LNCaP (AR +ve) and PC-3 (AR -ve) were used. MCF-7 and MDA-MB-231 cells were cultured in improved Dulbecco's modified Eagle's medium (IMEM), with glutamine and supplemented with 5% fetal bovine serum, 1% penicillin−streptomycin. T47D, LNCaP, and PC-3 cells were cultured in RPMI 1640 medium supplemented with 10% fetal bovine serum and 1% penicillin−streptomycin. Cells were grown as a monolayer in T75 or T150 tissue culture flasks in a humidified incubator (5% CO2, 95% air) at 37 °C.

ATRA Metabolism Assay. ATRA Metabolism Induction and Inhibition. MCF-7 and T47D cells (1×10^6 cells per 1 mL per well) were seeded in 6 well plates (Corning Costar plates). Cells were treated with 1 μM ATRA for 12−15 h to induce the cytochrome P450 enzyme. Cells were then washed with PBS and media and then incubated with different concentrations (0.0001−10 μM) of RAMBAs as well as with 0.001 μM [11,12 ^{3}H]-ATRA for a further period of 5 h (all of the drugs were dissolved in 95% ethanol to make the stock solution). The media and the trypsinized cells were then collected in glass tubes; radiolabed ATRA and metabolites were then extracted using ethyl acetate (with 10% methanol and 0.05% BHA). The extracted samples were dried and analyzed by reverse phase HPLC as described above.

Cell Growth Inhibition Assay (MTT Colorimetric Assay). Breast Cancer Cells. MCF-7 and T47D cells (1×10^4 cells per well per 1 mL of medium) were seeded in 24 well plates (Corning Costar plates). Cells were allowed to adhere to the plates for about 18 h and then treated with different concentrations (0.0001−10 μM) of drug (ATRA, and/or the RAMBAs dissolved in 95% ethanol) for 6 days, with renewal of media and drug on day 4. On day 7, medium was renewed and 100 μL of MTT (3-(4,5-dimethylthiazol-2-yl)-2,5-diphenyl-2*H*-tetrazolium bromide from Sigma) solution (5 mg MTT/mL of PBS) was added to the medium such that the ratio of MTT: medium was 1:10. The cells were incubated with MTT for 2 h. The medium was aspirated and 500 μL of DMSO was added to solubilize the blue-violet MTT-formazan product. The absorbance at 540 nm was measured by spectrophotometery (Victor 1420 multilabel counter, Wallac). For each concentration of the drug there were triplicate wells in every individual experiment. The data presented are mean ± SEM for 2−3 experiments. IC_{50} values were calculated by nonlinear regression analysis using Prism GraphPad software.

Prostate Cancer Cells. To measure cell viability, 24-well plates were coated with a 0.001% poly-L-lysine solution for 30 min. The wells were then washed with sterilized dH_2O. 1×10^4 LNCaP cells were seeded in the plates and maintained in RPMI 1640 medium. The cells were allowed to attach for 36 h. 1×10^4 PC-3 cells were seeded without poly-L-lysine treatment in the plates and maintained in RPMI 1640 medium. The cells were allowed to attach for 24 h. After attachment, fresh medium was added, and the cells were treated with a concentration range of either ATRA or one of the RAMBAs for 6 days. The medium was changed every 3 days. Cell were then treated with MTT and analyzed as described above.

Apoptosis APO-BRDU (TUNEL Assay). Apoptosis was determined by APO-BRDU (TUNEL assay) kit from "Pharmingen" and analyzed by flow cytometery. MCF-7 and T47D cells were treated with 1 μM ATRA, RAMBAs, and liarozole for 6 days in T75 flasks. Treated and untreated control cells were trypsinized, and $(1-2) \times 10^6$ cells were suspended in 0.5 mL of PBS. Cells were fixed with 1% w/v of paraformaldehyde and then again washed with PBS, suspended, and then stored overnight at −20 °C in 70% ethanol. Cells were then treated with DNA labeling solution consisting of TdT enzyme and BrdUTP. Next the cells were treated with fluorescein labeled anti-BrdU (antibody) and PI/RNase. Fluorescein labeled apoptotic cells were determined by flow cytometric analysis.

Differentiation Assay. LNCaP cells were incubated in the RPMI 1640 medium preparation containing 1 μM ATRA alone or in combination with a 1 μM concentration of one of the RAMBAs (**6** and **11**) for 6 days. LNCaP cells were scraped, and cell lysates were prepared. Fifty micrograms of cell lysate was run on a 10% SDS−PAGE gel at 90 V at room temperature. The separated lysates on 10% SDS−PAGE gel were transferred onto nitrocellulose membrane (Hybond ECL) overnight at 20 V at 4 °C. Western blot analysis was performed on the nitrocellulose membrane. The membrane was blocked for 1 h in 5% nonfat dried milk and PBS containing 0.5% Tween 20 (PBS-T) at room temperature. Following washing in PBS-T, the membrane was incubated with mouse monoclonal IgG antibody to cytokeratin 8/18 or β-actin (Santa Cruz Biotechnology and Oncogene, respectively) dissolved in 5% nonfat dried milk (1:5000 or 1:1000, respectively) for 1 h at room temperature. Following washing, the membrane was incubated with horseradish peroxidase linked sheep anti-mouse IgG antibody (Amersham and Oncogene, respectively) dissolved in 5% nonfat dried milk (1:1000) for 1 h at room temperature. The membrane was incubated in 4 mL ECL Western blotting analysis system (Amersham) for 1 min. The membrane was resolved on chemiluminescence film (Amersham Hyperfilm high performance chemiluminescence film), and the film was developed using an X-ray developer. The intensity of the bands on film was analyzed using ImageQuant 5.0 software (Amersham). The band intensity corresponds to the level of protein expression of cytokeratin 8/18, which is expressed in differentiated cells of epithelial origin.[45]

Retinoid Binding Assays. The IC_{50} values of each compound for RARα, RARβ, and RARγ were determined essentially as previously described using recombinant S-Tag RAR fusion proteins.[48−52] Binding assays were performed with receptor extracts diluted with binding buffer (40 mM HEPES, pH 7.9, 120 mM KCl, 10% glycerol, 0.1% (w/v) gelatin, 1 mM EDTA, 4 mM dithiothreitol (DTT), and 5 μg/mL each of the protease inhibitors aprotinin and leupeptin) to a final concentration of 10−30 μg/mL of total protein (0.1−0.3 pmol). [^{3}H]-*all-trans*-RA (1 nM) (1.82−1.92 TBq/mmol or 49.2−52.0 Ci/mmol; DuPont NEN) and various concentrations of each RAMBA (0−500 nM) were added to the binding reaction and incubated for 3 h at 27 °C. Nonspecific binding was determined in the presence of a 200-fold molar excess of unlabeled *all-trans*-RA. Bound RA was separated from free by extraction with 3% (w/v) equal particle size charcoal−dextran. All steps in the procedure were performed under yellow light. Specific RA binding was determined by subtracting the nonspecific binding, always less than 12% of the total binding, from the total binding. The IC_{50} value for each RAR subtype represents the RAMBA concentration that resulted in 50% inhibition of the binding of *all-trans*-RA. All binding assays were repeated at least three times.

In Vivo Antitumor Studies (MCF-7 Human Mammary Carcinoma Xenograft Model). All animal studies were performed according to the guidelines and approval of the

Animal Care Committee of the University of Maryland School of Medicine. Female ovariectomized athymic nude mice 4−6 weeks of age were obtained from the National Cancer Institute−Frederick Cancer Research and Development Center (Frederick, MD). The mice were maintained in a controlled environment with food and water supply.

Estrogen pellets (1.7 mg/pellet, 90 day continuous release obtained from Innovative Research of America) were implanted in the dorsal interscapular region of the mice using a trochar to facilitate tumor growth. Mice were then inoculated with MCF-7 cells (2×10^6 cells in Matrigel per tumor growth site) subcutaneously at one site on the right and left flanks. Tumors were allowed to grow for about 4−5 weeks till they were of measurable size (200−300 mm^3). The mice were then assigned to groups ($n = 5$) so that the total tumor volume was similar in each group. Treatment was then started, with compound **6** and ATRA formulated in 0.3% HPC (dose: 0.033 μmol/kg once a day, 6 days per week, 200 μL sc injection). Once every week the mice were weighed and tumors were measured using a caliper. Tumor volume was calculated according to the formula $(4/3)\pi r_1^2 r_2$ ($r_1 < r_2$). The tumor treatment study was continued for 6 weeks. At the end of 6 weeks, the mice were sacrificed and the tumors were collected, weighed, and stored until required.

Acknowledgment. This research was supported by grants from the U.S. Department of Defense under the Peer Review Medical Research Program (W81XWH-04-1-0101), the U.S. Army Medical Research and Material Command (DAM D17-01-1549), and TEDCO to V.C.O.N. C.H. was supported in part by NIH Grant NIEHS T32-ES07263. We thank all these agencies for their generous support. We are also grateful to Professor Gary H. Posner, Department of Chemistry, The Johns Hopkins University, Baltimore, for help with optical rotation measurements, and Dr. Gary Strahan, Department of Pharmaceutical Sciences, Scholl of Pharmacy, University of Maryland, Baltimore (UMB), for acquisition of some of ^{1}H and ^{13}C NMR data.

Supporting Information Available: Experimental details for preparation of intermediate compounds **3** and **4** and for preparation of compounds **13** and **14**. Procedure for statistical analysis, Lineweaver−Burk analysis plot (Figure A), and representative competition of [^{3}H]ATRA by RAMBAs (Figure B). This material is available free of charge via the Internet at http://pubs.acs.org.

References

(1) Mangelsdorf, D. A.; Umesono, K.; Evans, R. M. In *The Retinoids*; Sporn, M. B., Roberts, A. B., Goodman, D. S., Eds.; Raven Press: New York, 1994; pp 319−349.
(2) Mundi, J.; Frankel, S. R.; Miller, W. H., Jr.; Jakubowski, A.; Scheinberg, D. A.; Young, C. W.; Dmitrovski, E.; Warrell, R. P., Jr. Continuous treatment with all-*trans*-retinoic acid causes a progressive reduction in plasma drug concentrations: implications for relapse and retinoid 'resistance' in patients with acute promyelocytic leukemia. *Blood* **1992**, *79*, 299−303.
(3) Mundi, J.; Scher, H. I.; Rigas, J. R.; Warrell, R. P., Jr.; Young, C. W. Elevated plasma lipid peroxide content correlates with rapid plasma clearance of all-*trans*-retinoic acid in patients with advanced cancer. *Cancer Res.* **1994**, *54*, 2125−2128.
(4) Lee, J. S.; Newman, R. A.; Lippman, S. M.; Huber, M. H.; Minor, T.; Raber, M. N.; Krakoff, I. H.; Hong, W. K. Phase 1 evaluation of all-trans-retinoic acid in adults with solid tumors. *J. Clin. Oncol.* **1993**, *11*, 959−966.
(5) Miller, W. H., Jr. The emerging role of retinoids and retinoic acid metabolism blocking agents in the treatment of cancer. *Cancer* **1998**, *83*, 1471−1482.
(6) Njar, V. C. O. Cytochrome P450 retinoic acid 4-hydroxylase inhibitors: Potential agents for cancer therapy. *Mini-Rev. Med. Chem.* **2002**, *2*, 261−269.
(7) Freyne, E.; Raeymaekers, A.; Venet, M.; Sanz, G.; Wouters, W.; De Coster, R.; Van Wauwe, J. Synthesis of Liazal™, a retinoic acid metabolism blocking agent (RAMBA) with potential clinical applications in oncology and dermatology. *Bioorg. Med. Chem. Lett.* **1998**, *8*, 267−272.
(8) Thacher, S. M.; Vasudenvan, J.; Tsang, K.-Y.; Nagpal, S.; Chandraratna, R. A. S. New dermatological agents for the treatment of psoriasis. *J. Med. Chem.* **2001**, *44*, 287−296.
(9) Frolik, C. A.; Roberts, A. B.; Tavala, T. E.; Roller, P.; Newton, D. L.; Sporn, M. B. *Biochemistry* **1979**, *18*, 2092−2097.
(10) Nadin, L., Murray, M. Participation of CYP2C8 in retinoic acid 4-hydroxylation in hepatic microsomes. *Biochem. Pharmacol.* **1999**, *58*, 1201−1208.
(11) McSorley. L. C.; Daly, A. K. Identification of human cytochrome P450 isoforms that contribute to all-trans-retinoic acid 4-hydroxylation. *Biochem. Pharmacol*. **2000**, *60*, 517−526.
(12) Marill, J.; Cresteil, T.; Lanotte, M.; Chabot, G. G. Identification of human cytochrome P450 involved in the formation of all-trans-retinoic acid principal products. *Mol. Pharmacol.* **2000**, *58*, 1341−1348.
(13) White, J. A.; Guo, Y.-D.; Baetz, K.; Beckett-Jones, B.; Bonasoro, J.; Hsu, K. E.; Dilworth, F.; Jones, G.; Petkovich, M. Identification of the retinoic acid-inducible all-*trans*-retinoic acid 4-hydroxylase. *J. Biol. Chem.* **1996**, *271*, 29922−29927.
(14) White, J. A.; Beckett-Jones, B.; Guo, Y.-D.; Dilworth, F. J.; Bonasoro, J.; Jones, G.; Petkovich, M. cDNA cloning of human retinoic acid metabolizing enzyme (hP450RAI) identifies a novel family of cytochromes P450 (CYP26). *J. Biol. Chem.* **1997**, *272*, 18538−18541.
(15) Ray, W. J.; Bain, G.; Yao, M.; Gottlieb, D. I. CYP26, a novel mammalian cytochrome P450 is induced by retinoic acid and defines a new family. *J. Biol. Chem*. **1997**, *272*, 18702−18708.
(16) Abu-Abed, S. S.; Beckett, B. R.; Chiba, H.; Chithalen, J. V.; Glenville, J.; Metzger, D.; Chambon, P.; Petkovich, M. Mouse P450RAI (CYP26) expression and retinoic acid-inducible retinoic acid metabolism in F9 cells are regulated by retinoic acid receptor γ and retinoid X receptor α. *J. Biol. Chem.* **1998**, *273*, 2409−2415.
(17) Sonneveld, E.; Van der Sagg, P. T. Metabolism of retinoic acid: implications for development and cancer. *Int. J. Vitam. Nutr. Res.* **1998**, *68*, 404−410.
(18) Marill, J.; Idres, N.; Capron, C. C.; Nguyen, E.; Chabot, G. G. Retinoic acid metabolism and mechanism of action: A review. *Curr. Drug Metab.* **2003**, *4*, 1−10.
(19) Bhat, P. V.; Lacroix, A. Metabolism of retinal and retinoic acid in N-methyl-N-nitrosourea-induced mammary carcinomas in rats. *Cancer Res.* **1989**, *49*, 139−144.
(20) Wouters, W.; Van Dun, J.; Dillen, A.; Coene, M.-C.; Cools, W.; De Coster, R. Effects of liarozole, a new antitumoral compound on retinoic acid-induced inhibition of cell growth and on retinoic acid metabolism in MCF-7 breast cancer cells. *Cancer Res.* **1992**, *52*, 2841−2846.
(21) Krekels, M. D. W. G.; Zimmerman, J.; Janssen, B.; Van Ginckel, R.; Van Hove, C.; Coene, M.-C.; Wouter, W. Analysis of the oxidative catabolism of retinoic acid in rat Dunning R 3327G prostate tumors. *Prostate* **1996**, *29*, 36−41.
(22) Han, I. S.; Choi, J.-H. Highly specific cytochrome P450-like enzynes for all-trans-retinoic acid in T47D human breast cancer cells. *J. Clin. Endocrinol. Metab*. **1996**, *81*, 2069−2075.
(23) Krekels, M. D. W. G.; Verhoeven, A.; van Dun, J.; Cools, W.; Van Hove, C.; Dillen, L.; Coene, M.-C.; Wouters, W. Induction of oxidative catabolism of retinoic acid in MCF-7 cells. *Br. J. Cancer* **1997**, *75*, 1098−1104.
(24) Van der Leede, J., Van der Brink, C. E., Pijnappel, W. M.; Sonneveld, E.; Van der Saag, P. T.; Van der Burg, B. Autoinduction of retinoic acid metabolism to polar derivatives with decreased biological activity in retinoic acid-sensitive, but not in retinoic acid-resistant breast cancer cells. *J. Biol. Chem.* **1997**, *272*, 17921−17928.
(25) Sonneveld, E.; Van der Brink, C. E.; Van der Leede, B. M.; Schulkes, R. A. M., Petkovich, M.; Van der Burg, B.; Van der Saag, P. T. Human retinoic acid (RA) 4-hydroxylase (CYP26) is highly specific for all-trans-RA and can be induced through RA receptor in human breast and colon carcinoma cells. *Cell Growth Differ.* **1998**, *9*, 629−637.
(26) Van Heusden, J.; Van Ginckel, R.; Bruwiere, H.; Moelans, P.; Janssen, B.; Floren, W.; Van der Leede, B. J.; Van Dun, J.; Sanz, G.; Venet, M.; Dillen, L.; Van Hove, C.; Willemsens, G.; Janicot, M.; Wouters, W. Inhibition of all-*trans*-retinoic acid metabolism by R116010 induces antitumor activity. *Br. J. Cancer* **2002**, *86*, 605−611.
(27) Stoppie, P.; Borgers, M.; Borghgraef, P.; Dillen, L.; Goossens, J.; Sanz, G.; Szel, H.; Van Hove, C.; Van Nyen, G.; Nobels, G.; Vanden Bossche, H.; Venet, M.; Willemsens, G.; Van Wauwe, J. R115866 Inhibits all-trans-retinoic acid metabolism and exerts retinoidal effects in rodents. *J. Pharmacol. Exp. Ther.* **2000**, *293*, 304−312.
(28) Vasudevan, J.; Johnson, A. T.; Huang, D.; Chandraratna, R. A. Compounds having activity as inhibitors of cytochrome P450A1. US Patent. 6,252,090. Other patents assigned to Allergan Sales, Inc., include US Patents 6,303,785 B1; 6,313,107 B1; 6,359,135 B1; 6,369,261 B1; 6,380,256 B1; 6,387,892 B1; 6,387,951 B1; 6,-399,774 B1; 6,495,552 B2; and 531,599 B2.

(29) (a) Kirby, A. J.; Lelain, R.; Mason, P.; Maharlouie, F.; Nicholls, P. A.; Smith, H. J.; Simons, C. Some 3-(4-aminophenyl)pyrrolidine-2,5-diones as all-trans-retinoic acid metabolising enzyme inhibitors (RAMBAs). *J. Enzyme Inhib.* **2002**, *17*, 321−327. (b) Greer, V. P.; Mason, P.; Kirby, H. J.; Smith, H. J.; Nicholls, P. A.; Simons, C. Some 1,2-diphenylethane derivatives as inhibitors of retinoic acid-metabolising enzymes. *J. Enzyme Inhib.* **2003**, *18*, 431−443. (c) Mason, P.; Greer, V. P.; Kirby, A. J.; Simons, C.; J.; Nicholls, P. A.; Smith, H. Some aryl substituted 2-(4-nitrophenyl)-4-oxo-4-phenylbutanoates and 3-(4-nitrophenyl)-1-phenyl-1,4-butanediols and related compounds as inhibitors of rat liver microsomal retinoic acid metabolising enzymes. *J. Enzyme Inhib.* **2003**, *18*, 511−528.

(30) (a) Njar, V. C. O.; Nnane, I. P.; Brodie, A. M. H. Potent inhibition of retinoic acid metabolism enzyme(s) by novel azolyl retinoids. *Bioorg. Med. Chem. Lett.* **2000**, *10*, 1905−1908. (b) Njar, V. C. O.; Patel, J.; Huynh, C. K.; Handratta, V.; Brodie, A. M. H. Synthesis of new inhibitors of all-trans-retinoic acid metabolism and their effects on proliferation of human breast cancer cells. *Proceedings of the The Department of Defense Breast Cancer Research Program Meeting (Era of Hope)*, Orlando, FL, Sept 25−28, 2002; Abstract No. P31-17. (c) Patel, J.; Brodie, A. M. H.; Njar, V. C. O. New 4-azolyl retinoids (retinoic acid metabolism blocking agents): Emerging candidates for breast cancer chemoprevention and therapy. *Proceedings of American Association for Cancer Research, 95th Annual Meeting*, March 27−31, 2004, Orlando, FL; Abstract No. 5604. (d) Huynh, C. K.; Brodie, A. M. H.; Njar, V. C. O. Retinoic acid metabolism blocking agents as a potential treatment for prostate cancer. *Proceedings of the Endocrine Society's 86th Annual Meeting*, New Orleans, LA, June 16−19, 2004; Abstract No. P1-269, pp 219.

(31) Hashimoto, N.; Aoyama, T.; Takayuki, S. New methods and reagents in organic synthesis. 14. A simple efficient preparation of methyl esters with trimethylsilyldiazomethane ($TMSCHN_2$) and its application to gas chromatographic analysis of fatty acids. *Chem. Pharm. Bull* **1981**, *29*, 1457−1477.

(32) Samokyszyn, V. M.; Gall, W. E.; Zawada, G.; Freyaldenhoven, M. A.; Chen, G.; Mackenzie, P. I.; Tephyl, T. R.; Radominska-Pandya, A. 4-Hydroxyretinoic acid, a novel substrate for human liver microsomal UDP-glycuronosyltansferase(s) and recombinant UGT2B7. *J. Biol. Chem.* **2000**, *275*, 6908−6914.

(33) Totleben, M. J.; Freeman, J. P.; Szmuszkovica, J. Imidazole transfer from 1,1′-carbonyldiimidazole and 1,1′-(thiocarbonyl)-diimidazole to alcohols. A new protocol for the conversion of alcohols to alkylheterocycles. *J. Org. Chem.* **1997**, *62*, 7319−7323.

(34) (a) Englert, G. A 13C-NMR. Study of cis-trans isomeric vitamins A carotenoids and related compounds. *Helv. Chim. Acta* **1975**, *58*, 2367−2390. (b) Dawson, M. I.; Hobbs, P. D.; Kuhlmann, K.; Fung, V. A.; Helmes, C. T.; Chao, W. Retinoic acid analogues. Synthesis and potential as cancer chemopreventive agents. *J. Med. Chem.* **1980**, *23*, 1013−1022.

(35) Shealy, Y. F.; Riordan, J. M.; Frey, J. L.; Simpson-Herren, L.; Sani, B. P.; Hill, D. L. Inhibition of papilloma formation by analogs of 7,8-Dihydroretinoic acid. *J. Med. Chem.* **2003**, *46*, 1931−1939.

(36) Katsuta, Y.; Ito, M.; Yoshihara, K.; Nakanishi, K.; Kikkawa, T.; Fujiwara, T. Synthesis of (+)-(4S)- and (−)-(4R)-(11Z)-4-hydroxyretinals and determination of the absolute stereochemistry of a visual pigment chromophore in the firefly squid, *Watasenia scintillans. J. Org. Chem*. **1994**, *59*, 6917−6921.

(37) Taimi, M.; Breitman, T. R. *N*-4-Hydroxyphenylretinamide enhances retinoic acid-induced differentiation and retinoylation of proteins in the human acute promyelocytic leukemia cell line, NB4, by a mechanism that may involve inhibition of retinoic acid metabolism. *Biochem. Biophys. Res. Commun*. **1997**, *232*, 432−436.

(38) Roberts, A. B.; Lamb, L. C.; Sporn, M. B. Metabolism of all-trans-retinoic acid in hamster liver microsomes. Oxidation of 4-hydroxy to 4-keto-retinoic acid. *Arch. Biochem. Biophys.* **1980**, *199*, 374−383.

(39) Van Wauwe, J. P.; Coene, M.-C.; Goossens, J.; Van Nyen, G.; Cools, W.; Lauwers, W. Ketoconazole inhibits the in vitro and in vivo metabolism of all-trans-retinoic acid. *J. Pharmacol. Exp. Ther.* **1988**, *245*, 718−722.

(40) Kim, S. Y.; Kim, C.; Han, I. S.; Lee, S. C.; Kim, S. H.; Lee, K., Choi, Y.; Byun, Y. Inhibition effect of new farnesol derivatives on all-*trans*-retinoic acid metabolism. *Metabolism* **2001**, *50*, 1356−1360.

(41) Botta, M.; Corelli, F.; Gasparrini, F.; Messina, F.; Mugnaini, C. Chiral azole derivatives. 4. Enantiomers of bifonazole and related antifungal agents: Synthesis, configuration assignment, and biological evaluation. *J. Org. Chem.* **2000**, *65*, 4736−4739.

(42) Mosmann, T. Rapid colorimetric assay for cellular growth and survival: application to proleferation and cytotoxicity assays. *J. Immunol. Methods* **1983**, *65*, 55−63.

(43) Idres, N.; Marill, J.; Flexor, M. A.; Chabot, G. G. Activation of retinoic acid receptor-dependent transcription by all-*trans*-retinoic acid metabolites and isomers. *J. Biol. Chem.* **2002**, *277*, 31491−31498.

(44) Gavrieli, Y.; Sherman, Y.; Ben-Sasson, S. A. Identification of programmed cell death in situ via specific labeling of DNA fragmentation. *J. Cell Biol.* **1992**, *119*, 493−502.

(45) Hsieh, T. C.; Xu, W.; Chiao, J. W. Growth regulation and cellular changes during differentiation of human prostatic cancer LNCaP cells as induced by T lymphocyte-conditioned medium. *Exp. Cell Res.* **1995**, *218*, 137−143.

(46) Hall, A. K. Liarozole amplifies retinoid-induced apoptosis in human prostate cancer cells. *Anti-Cancer Drugs* **1996**, *7*, 312−320.

(47) Njar, V. C. O. High-yield synthesis of novel imidazoles and triazoles from alcohols and phenols. *Synthesis* **2000**, *14*, 2019−2028.

(48) Scafonas, A.; Wolfgang, C. L.; Gabriel, J. L.; Soprano, K. J.; Soprano, D. R. Differential role of homologous positively charged residues for ligand binding in retinoic acid receptor compared with retinoic acid receptor. *J. Biol. Chem.* **1997**, *272*, 11244−11249.

(49) Zhang, Z.-P.; Gambone, C. J.; Gabriel, J. L.; Wolfgang, C. L.; Soprano, K. J.; Soprano, D. R. Arg^{278}, but not Lys^{229} or Lys^{236}, plays an important role in the binding of retinoic acid by retinoic acid receptor. *J. Biol. Chem.* **1998**, *273*, 4016−4021.

(50) Zhang, Z.-P.; Shukri, M.; Gambone, C. J.; Gabriel, J. L.; Soprano, K. J.; Soprano, D. R. Role of Ser^{289} in RARγ and its homologous amino acid residue of RARα and RARβ in the binding of retinoic acid. *Arch. Biochem. Biophys*. **2000**, *380*, 339−346.

(51) Wolfgang, C. L.; Zhang, Z.-p.; Gabriel, J. L.; Pieringer, R. A.; Soprano, K. J.; Soprano, D. R. Identification of sulfhydryl-modified cysteine residues in the ligand binding pocket of retinoic acid receptor β. *J. Biol. Chem.* **1997**, *272*, 746−753.

(52) Zhang, Z. P.; Hutcheson, J. M.; Poynton, H. C.; Gabriel, J. L.; Soprano, K. J.; Soprano, D. R. Arginine of retinoic acid receptor β which coordinates with the carboxyl group of retinoic acid functions independent of the amino acid residues responsible for retinoic acid receptor subtype ligand specificity. *Arch. Biochem. Biophys.* **2003**, *409*, 375−384.

JM0401457